NAZARBAYEV UNIVERSITY

School of Engineering and Digital Sciences

Bachelor of Engineering in

Mechanical and Aerospace Engineering

Design and Development of a Rotating Nozzle for Large-Scale Construction 3D Printer

(Final Report for Capstone Project)

by

Akbota Uskembayeva
Bakhytgul Sarsenova
Ramazan Dursunov

Supervisors: Associate Professor Md. Hazrat Ali,
Professor Essam Shehab

April 2025

Declaration

We hereby declare that this report entitled “Design and Development of a Rotating Nozzle for Large-Scale Construction 3D Printer” is the result of our own project work except for quotations and citations that have been duly acknowledged. We also declare that it has not been previously or concurrently submitted for any other degree at Nazarbayev University.

Akbota Uskembayeva

Bakhytgul Sarsenova

Ramazan Dursunov

Date: April 28, 2025

Acknowledgements

We would like to express our deepest gratitude to our supervisors Professor Md. Hazrat Ali and Professor Essam Shehab for their valuable guidance in completing this capstone project.

We want to express our special thanks to our research team for the project “Sustainable Construction 3D Printing: Utilization of Kazakhstan's Industrial Waste and Green Cement” for providing necessary facilities required for the project.

We want to thank all our friends and family members for their valuable support and motivation throughout the process of accomplishing this project.

Abstract

This capstone project focuses on the design and control system of a rotating nozzle for 3D construction printers. The existing 3D construction printer at Nazarbayev University is equipped only with a stationary nozzle with a circular cross-section which does not allow the use of a non-circular nozzle due to the lack of a rotational mechanical system in the printer itself. This, in turn, limits the opportunity to effectively enhance mechanical properties such as tensile and compressive strengths. The proposed design is developed through computer aided design (CAD) software and the printer's configuration is adjusted for integration of the rotational mechanism's control system. This design includes a full description of rotational mechanism and integration steps to the 3D printer. Besides the main motor of the 3D printer, an additional motor is installed next to the nozzle and controlled by a new axis (parameter) which is added into G-code. New axis, called "U", will be responsible for rotation of the nozzle itself. For the development of this axis design, the cosine law is applied. The calculation is based on the three consecutive points in G-code to obtain an accurate degree of rotation for the nozzle. Based on testing results one trowel printhead had the highest flexural strength of 5 MPa and a trapezoidal printhead with teeth had the highest compressive strength of 8 MPa compared to circular default nozzle head with 6 MPa and 2 MPa for compressive and flexural strengths respectively. The new optimized nozzle design is implemented in existing 3D printers, which allows it not only to develop its capability in the printing process but also to make sustainable contributions in 3D construction industries.

Table of contents

List of Figures

List of Tables

List of Publications

A. Uskembayeva, B. Sarsenova, R. Dursunov, B. Temirzakuly, E. Shehab, and M. H. Ali, “Design and development of a rotating nozzle for large-scale construction 3D printer,” in Proc. Int. Conf. on Smart Advanced Manufacturing (ICSAM), Univ. of Malaya, Kuala Lumpur, Malaysia, 2024..

Chapter 1: Introduction

1.1 Background

3D printing technologies are innovative and advanced methods of manufacturing which can be implemented in different areas. It allows the creation of complex geometric shapes and structures using layering of material (Rasiya et al., 2021). As a result, with rapid population growth and the requirement of popularization of green technologies, 3D printing might be highly effective in large-scale construction. Because large-scale 3D printing has advantages over traditional construction such as less dependence on labor, complex-shaped construction and environmentally effective building (Xiao et al., 2021). Thus, nowadays there is a high need for development of large scale 3D construction printers that use green material for extrusion which will have more durability compared to traditional construction's.

1.1.1 Geopolymer

Geopolymer technology is revolutionary in the production of eco-friendly building materials. These inorganic polymers are synthesized from aluminosilicate-rich precursors that are activated by alkalis, for example, fly ash, metakaolin, and blast furnace slag (Duxson et al., 2007). For the development of a three-dimensional network of aluminosilicate, silicon and aluminum species are dispersed in an alkaline medium and then get polycondensed to develop a rigid gel structure with improved mechanical and chemical characteristics (Duxson et al., 2007; Cong & Cheng, 2021). The geopolymers found a great use in the construction industry as well as industrial processing because of their properties, for example, low heat conductivity, durability, acid and fire resistance, and high compressive strength (Almutairi et al., 2021).

Sustainable performance is propelling innovation in geopolymers to a significant level. Cement of the conventional type is linked to large emissions of greenhouse gas (GHG), which is approximately 6–8% of global anthropogenic CO_2 production (Almutairi et al., 2021). Geopolymers, on the other hand, are associated with up to 80% reduction of embodied carbon that depends on used feedstock and alkali activators (Almutairi et al., 2021). Because the majority of geopolymer precursors are industrial waste products, such as fly ash, red mud, and slag, they are especially alluring because they conserve both waste and natural resources (Cong & Cheng, 2021). Furthermore, they use less energy to produce than traditional cement, which improves environmental sustainability even more (Duxson et al., 2007).

Geopolymer's mechanical properties are directly correlated to the raw materials used and their treatment type. For instance, fly ash-based geopolymers have high cost-effectiveness and are easier to work with, while geopolymers based on metakaolin are incredibly pure and long-lasting (Cong & Cheng, 2021). Ground granulated blast furnace slag (GGBS) promotes early strength development and durability. Also noteworthy is the type and quantity of the alkali activator — typically a combination of sodium hydroxide (NaOH) and sodium silicate (Na_2SiO_3). Sodium silicate is critical to geopolymerization because it introduces soluble silica, which increases the Si/Al ratio, promotes gel formation, and improves mechanical strength (Duxson et al., 2007). This combination not only accelerates the dissolution of aluminosilicates but also accelerates the polycondensation reactions to form denser and more robust geopolymer matrices (Almutairi et al., 2021). Sodium activators dissolve silica and alumina more effectively than potassium systems, and thus they have enormous application (Cong & Cheng, 2021).

Structurally, geopolymers differ from cement in that their gel matrix consists of silicon and aluminum tetrahedra linked by oxygen atoms to create a highly cross-linked inorganic polymer network. This is the structure responsible for the material's chemical resistance and low permeability, making it suitable for aggressive environments. Improved techniques in electron microscopy and nuclear magnetic resonance (NMR) have revealed more about these materials and how small differences in composition affect gelation, pore structure, and long-term stability (Duxson et al., 2007).

1.1.2 Construction 3D Printer

In Nazarbayev University laboratory, there is a concrete 3D printer (Figure 1), which is used in the project “Sustainable Construction 3D Printing: Utilization of Kazakhstan's Industrial Waste and Green Cement”. During the two years of work on the project, many limitations were found that prevent an increase in compressive strength. One of these problems is the non-routability of the nozzle along its axis.

Figure 1: Concrete printer in NU

1.2 Research Motivation

The existing 3D construction printer at Nazarbayev University operates with a stationary nozzle of circular cross-section, which moves in accordance with X, Y, Z direction of printing (Figure 2) . The current problem is the incapability of the 3D printer nozzle to rotate. As a result, the printer can only be used with nozzles that have a circular cross-section; other forms, including rectangular cross-sections, cannot be used. This constraint limits the printer's adaptability because it is unable to support non-circular nozzle geometries, which could be useful for enhancing interlayer strength of printed material.

Figure 2: Stationary nozzle of circular cross-section

1.3 Aim and Objectives

The aim of the capstone project is to enhance the efficiency of 3D printing construction by the development of a nozzle rotation mechanism with implementation of non-circular nozzle shapes. It is expected that implementation of a rotating nozzle system where the nozzle head will rotate in accordance with changing printing direction, affects the quality of printed model.

The objectives of this project are to:

- Incorporate a reliable rotation control algorithm that ensures precise and smooth nozzle movement;
- Assess the impact of non-circular nozzles on the structural properties of printed elements;
- Compare mechanical properties of parts printed with different nozzle heads;
- Determine the nozzle head shape that produces printed parts with the best mechanical properties.

1.4 Capstone Report Structure

Chapter 1 - Introduction

The section presents the background of the 3D construction printing, establishes the research problem within the nozzle system, and determines the research aims and objectives.

Chapter 2 - Literature Review

This chapter presents a comprehensive overview of the past research papers on the topic of geopolymers, nozzle geometries and their effects on mechanical properties of printed mortar structures, as well as rotation mechanisms and their suitability for 3D printing technologies. These research works cover both theoretical part of the topics and empirical research done, the chapter highlights the limitations and advancements of the papers and their use for this capstone project report.

Chapter 3 - Methodology

This chapter addresses the methods of the product development and its testing. There are described processes that are considered to develop the prototype of the rotating nozzle system and the nozzle head shapes, decomposition material optimization for the new system, and the testing methods.

Chapter 4 - Results

This section reports the results of the mechanical system prototyping with integration to the 3D printer hardware basis. Also, there are represented 3D printing results of using different nozzle heads incorporated to the rotating nozzle system, with the results of its compressive and flexural strength.

Chapter 5 - Discussion and Analysis

This chapter analyzes the obtained results in achieving the aims. Specifically, there are discussed challenges with the project, the integration capability of the developed system, and the influence of the nozzle head shape to the printed model properties.

Chapter 6 - Conclusion and Future Research

This chapter demonstrates key findings and results obtained from the testing stage. Moreover, contribution to the development of 3D construction printing is specified there. For future investigation significant research directions such as optimization, efficiency and durability are mentioned in order to reach the full potential of 3D construction printers.

Chapter 2: Literature Review

2.1 Introduction

The emergence of 3D printing in the building industry has opened up new possibilities for improving building methods, cutting down on material waste, and precisely creating intricate structures. The nozzle design is critical to the success of large-scale 3D printing, especially in the construction sector, as it affects print quality, structural stability, and efficiency. To better understand how nozzle design, geometry, and optimization affect 3D printing performance, this literature review examines recent research in these areas. Extrudability, buildability, interlayer bonding, and surface polish are among the parameters that are specifically addressed since they are critical to the effective use of 3D printing in large-scale buildings.

2.2 Nozzle Criterias for Enhancing Material Properties in 3D Printing Concrete

In their thorough examination of nozzle parameters for 3D printing concrete, Yang et al. (2022) showed how important nozzle design is for enhancing extrudability, buildability, and interlayer bonding. The study examined more than 70 research papers on nozzle design and identified the four primary factors: nozzle travel speed, size, form, and distance from the build surface. These elements control the consistency of layer construction and the ease with which the layers adhere to one another.

Extrudability is significantly impacted by the nozzle's dimensions. Increased friction and clogs can result from smaller nozzle diameters, particularly when materials containing recycled aggregates are used. According to Yang et al., environmentally friendly nozzle design can save carbon footprints and improve the recyclability of building materials. Furthermore, the research highlighted that enhancing nozzle design may result in enhanced buildability, decreased material waste, and more consistent layer adhesion, hence rendering 3D printing a more feasible option for environmentally conscious buildings.

2.3 Design of Novel Nozzles for Higher Interlayer Strength

The research by He et al. (2021) explored the development of novel nozzle designs aimed at improving the interlayer bonding strength of 3D-printed cement paste. A combination of simulation and experimentation was used in this work to explore several nozzle geometries, such as circular, rectangular, and more intricate shapes like "Kidney." By maximizing the

geometry of the extruded material and reducing flaws such as interlayer notches, the "Kidney" nozzle, according to the authors, greatly increased interlayer strength. Some of the geometries that were used in the research are shown on Figure 3.

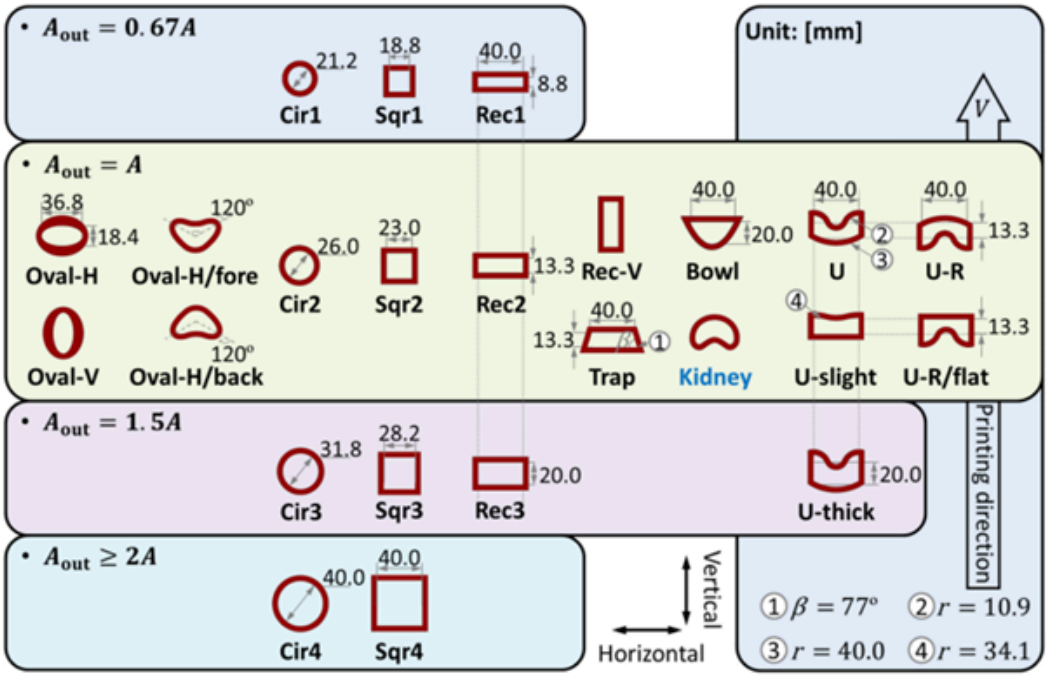

Figure 3: Shapes and geometries with dimensions used in work by He et al. (2021)

Apart from experimenting with various nozzle designs, the study presented novel nozzle components such as side trowels and interface shapers that are shown in Figure 4.

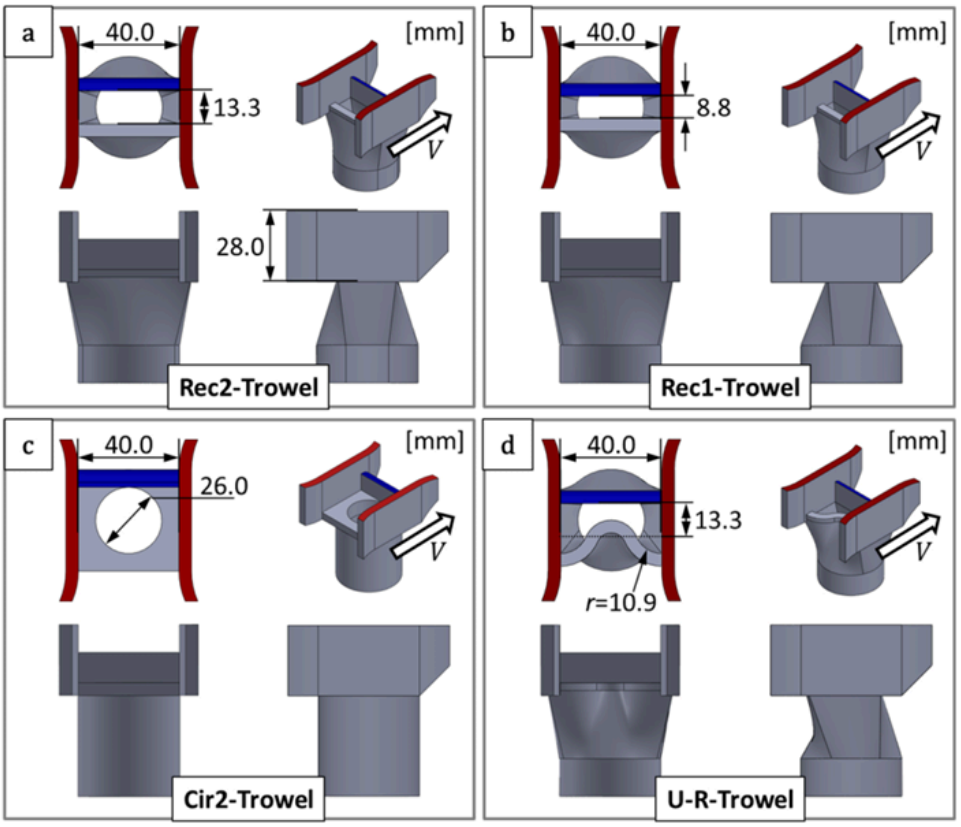

Figure 4: Examples of trowels (He et al., 2021)

These components will help to avoid notch formation and provide good adherence of the extruded material to the underlying layer, hence improving the quality of the interlayer connection. Accordingly, these components increased the interlayer bonding strength by twofold and showed that the optimization of the nozzle is essential for the improvement of mechanical performance in 3D-printed structures.

2.4 Effect of Different Nozzles Shapes and Fibre-Reinforcement in 3D Printed Mortar

The impact of fiber reinforcement and nozzle shape on the mechanical characteristics of 3D-printed mortar was investigated by Shakor et al. (2019). The effects of circular, oval, and rectangular nozzle geometries on the printability of fiber-reinforced cementitious materials were examined in this work. According to the results, fiber-reinforced mortar has substantially greater flexural and compressive strength than non-reinforced mortar when printed through nozzles that are specifically made for the purpose. The difference between the nominal and reduced widths of different layers for parts printed with circular and rectangular nozzles that were obtained by Shakor et al. (2019) are shown on Figure 5.

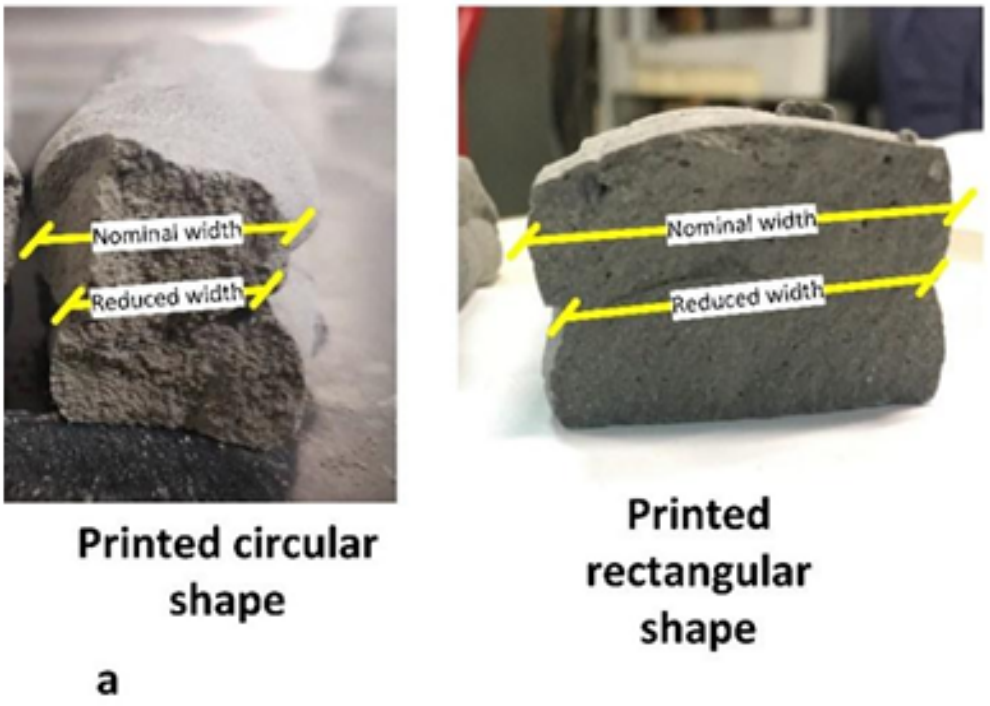

Figure 5: Reduced and nominal widths of parts (Shakor et al., 2019)

The study also showed that throughout the printing process, nozzle shape is crucial in ensuring that fiber-reinforced mortar is dispersed uniformly and aligned correctly. For example, it was discovered that rectangular nozzles distributed fiber-reinforced mortar more effectively, improving the structure's structural integrity and load-bearing capability. This study showed that the overall performance of 3D-printed objects can be enhanced by combining sophisticated material formulas with optimal nozzle designs.

First and foremost, new geometries in conjunction with extra elements like side trowels and interface shapers, can greatly improve interlayer bonding and structural stability. Secondly, the impact of nozzle geometry on the mechanical characteristics and surface polish of the printed structure needs to be carefully considered. For instance, depending on the printing stage and material parameters, a rotating nozzle may alternate between several shapes to maximize performance.

2.5 Effects of Nozzle Geometries on 3D Printing of Clay Constructs

Nozzle geometry plays a vital role in making 3D-printed objects work and be of quality. Manikandan et al. (2020) studied how contour deviation, surface roughness, and compression

strength were influenced by the use of a circular and square nozzle geometries in extrusion-based additive manufacturing. Their results show how nozzle design influences mechanical characteristics and surface quality.

This work used DIW technology to demonstrate that the use of circular nozzles made the layers align more consistently with a lot of smooth surfaces showing minimal contour deviations. With these attributes, the resultant parts could have various applications where an artistic level of finish is critical. Square nozzles increased compression strength greatly with a great likelihood of developing more pronounced layering artifacts, increasing the roughness of the surface topography. Square nozzles were more efficient in the case of structural and load-bearing components, since they produced flat-edged layers that improve load distribution.

Using point cloud data, quantitative analysis showed the trade-offs between strength and surface quality. Square nozzles offer more mechanical strength and endurance, whereas circular nozzles perform best in projects that prioritize aesthetics. The study highlights the necessity of choosing nozzles specifically for a project based on its requirements. Manikandan et al. (2020) further indicate that hybrid or adaptive nozzles might be designed, which can dynamically change their geometry during printing. This may enhance 3D printing's adaptability and effectiveness, opening wider uses in the building industry and beyond.

2.6 Steps of the Engineering Design Process

A methodical, iterative approach to engineering design is described in the article "What Are The 7 Steps Of The Engineering Design Process" by Big Bolt (2022). By determining the demands of the user and the resources needed, the design process starts with the first step which is defining the problem. As the second step, the research is then carried out to examine alternatives and all pre-existing concepts. Ideas are jointly generated to solve the problem in the third step of engineering design, Brainstorm & Conceptualize, and then concepts are evaluated and improved upon in the Prototype Creation step. Prototypes are evaluated at the Select & Finalize process, and the best one is chosen for full production. While improving product design adjusts to changing market trends and needs, product analysis guarantees continuous review. In order to stay competitive in ever-changing markets, this systematic methodology guarantees efficient problem-solving, user-focused solutions, and ongoing product enhancement.

Overall, there are seven steps of engineering design (Bolt, 2022). The developed project is novel for the academy, because it introduces engineering design and control systems for rotational mechanisms implemented to 3D construction printers for the first time. Thus, this project covers only the first 4 steps of engineering design which ends with creating a prototype. On the 4th stage, the concepts and assumptions will be tested and based on the results, corresponding minor adjustments will be made to the design for the optimization.

2.7 Conclusion

The literature review highlights nozzle design as one of the most critical aspects of large-scale 3D printing for construction. Some of the major aspects of print quality, structural integrity, and material performance are considerably influenced by nozzle size, shape, and travel speed. Nozzle design optimization will be of prime importance to achieve improved mechanical properties in the printed structures, reduced material wastage, and increased efficiency as 3D printing is a transformative technology in the construction industry. Building on this, a rotating nozzle has been developed that can address several challenges commonly faced in the large-scale 3D printing of construction materials. If ongoing research and improvements are made in nozzle design, then 3D printing can prove to be a game-changer for the construction sector in cost-effective and sustainable building.

Chapter 3: Methodology

3.1 Design Steps

The methodology of this capstone project report is based on the 7 step engineering design process described by the Big Bolt company (2022). The steps can be seen on the Figure 6 below:

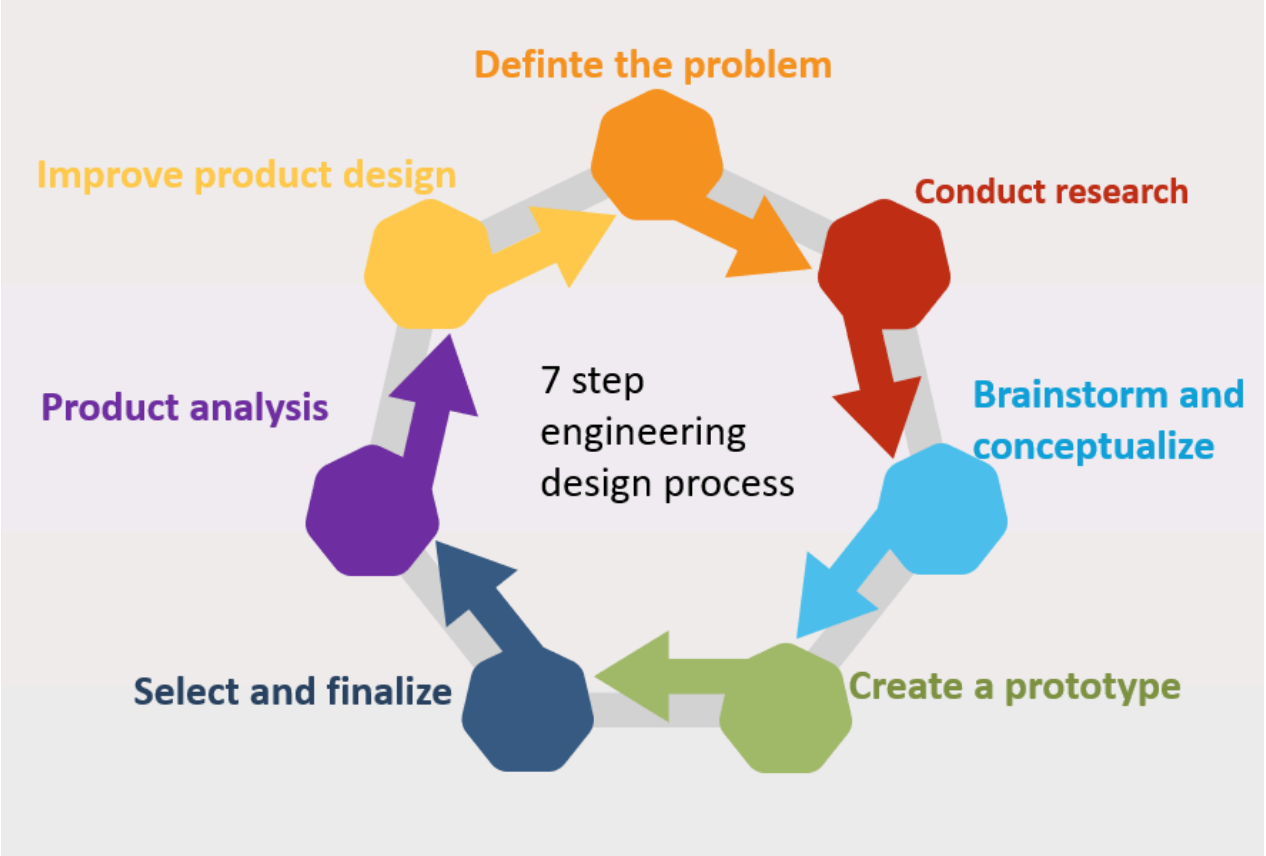

Figure 6: Design steps

The methodology section describes a systematic approach used to achieve objectives of the design and development of a rotating nozzle system for the large-scale 3D construction printer. The study consists of control algorithm development, mechanical design principles, material selection analysis, and experimental validation to ensure optimal nozzle performance and efficiency for improving the mechanical properties of printed parts.

3.2 Method Selection

For the limitations of the existing construction 3D printer two different research methods were chosen as the most effective, namely applied research and exploratory research. These two methods helped examine and analyze existing literature, current problems and develop

possible solutions. The aim was to come up with a functional prototype that would increase the adaptability and performance of the printer by solving the issues presented by stationary circular nozzles. Applied research is a practical way of finding a solution that was mainly used in order to prototype a rotational mechanical system that could be integrated to the existing 3D printer. As applied research is based on the development of tangible outcomes, it could be said that conceptualization and design of the system using CAD software, manufacturing of the system parts and their later assembly all fall into the applied research method.

Meanwhile, exploratory research method was greatly used in background knowledge development, procurement of basic information on the topic of rotational mechanisms and their implementations and applications in construction 3D printing, and analysis of the effects of different nozzle geometries. The presented topic of rotational mechanical systems for 3D printers is relatively new, and it highlights the importance of thorough evaluation of the current situation in order to achieve the best possible solution. As a part of exploratory research method, several studies were analyzed, including studies researching geopolymer, studies looking into different nozzle geometries and studies mentioning implementation of a rotating mechanism. As mechanical properties are one of the major aspects contributing to the accomplishment of the aims of the study, papers dealing with interlayer adhesion, compressive strength and material extrusion were also included as part of the exploratory research. Both research techniques gave a strong foundation for the project by combining them and tackling technical issues.

3.3 Mechanical System Design

For the conceptualization and development of the rotating nozzle mechanical system, the CAD software, namely SolidWorks was used. It allowed the detailed 3D CAD model of the proposed system design to be created based on the requirements set for the capstone project. It also provided the space to perform the analysis of the system to ensure the compatibility of the designed parts with the unique features of the existing construction 3D printer. The features included the dimensions and configurations of the used stationary circular nozzle. There was no need to redesign the whole proposed system, as SolidWorks software gave the opportunity to focus on separate parts and their adjustment.

In SolidWorks, both the rotating mechanism of the nozzle and a rectangular cross-section nozzle with integrated trowels were modeled with precision. The mechanical system for

rotation itself was engineered around a bearing system, with two meshing gears. A gear drive has been chosen over a belt drive owing to the superior characteristics a gear drive has in respect to performance, in particular the absence of any slipping, which is vital to obtaining a smooth and precise rotating action. To ensure a proper flow of torque from the stepper motor to the gears with operational reliability, the gear drive is designed around a 1:1 ratio gearbox. It balances simplicity with effectiveness.

For the bearing system, based on the basic dimensions of the existing extrusion nozzle system for the ease of assembly it was decided to use a 6007 type ball bearing. The use of press fit of the bearing into a custom-printed mandrel improved the stability and functionality of the whole mechanical system. With the bearing in its place in the mandrel, the mandrel itself can be installed to the upper adapter and fixed at one place using the snap ring. This was further reinforced by fixing the lower part of the nozzle directly to the mandrel with bolts. These choices of the coupling of different parts ensured the precise alignment and operation of the system, as well as simplicity of the assembly and disassembly of the nozzle system that is essential for future maintenance and possible modifications.

In order to support the stepper motor that is essential for the rotational movement of the nozzle system, a separate part with a mounting platform was introduced. The part was designed in the best possible manner so that the motor is perfectly aligned with the gearbox and bearing system. The motor mounting was important for the assembly, which provided the necessary rotational control so that the nozzle could dynamically change orientation in accordance with the printing specifications. From a more general perspective, these elements of the designed system have been carefully approached, and by doing so methodically, ensure that all goals of this project are met both in technological viability and in utility in expanding 3-D printing capability.

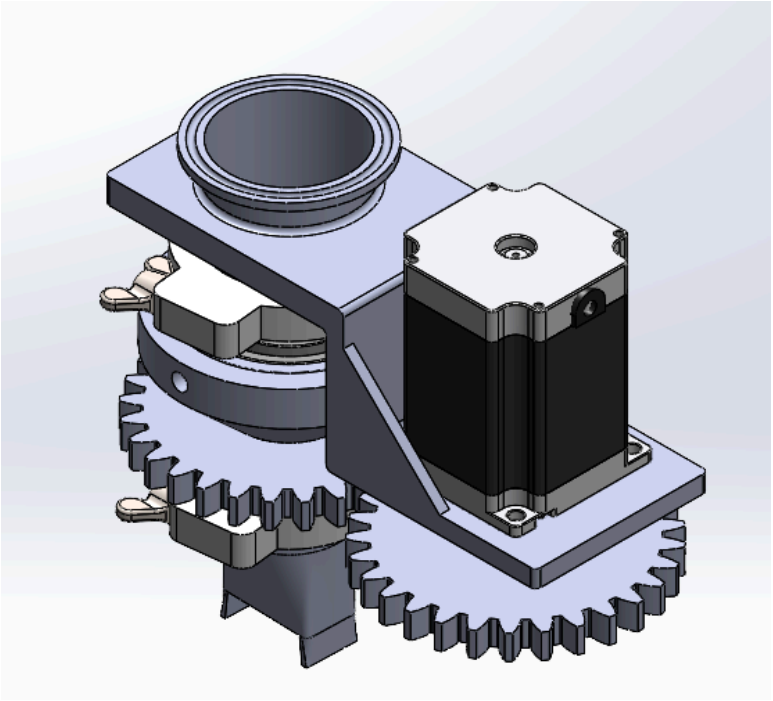

Figure 7: Proposed CAD model of the nozzle with a rotational mechanism

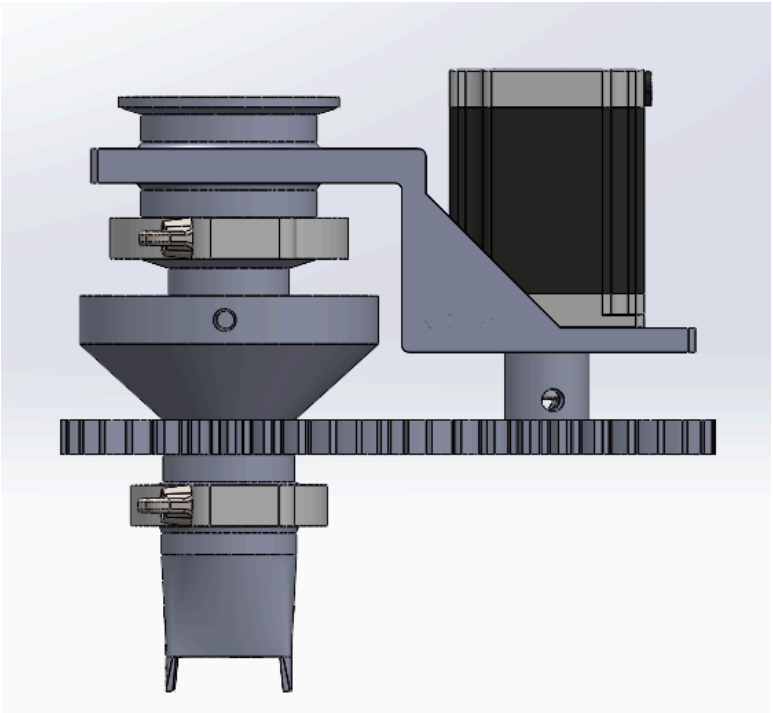

Figure 8: Front view of CAD model

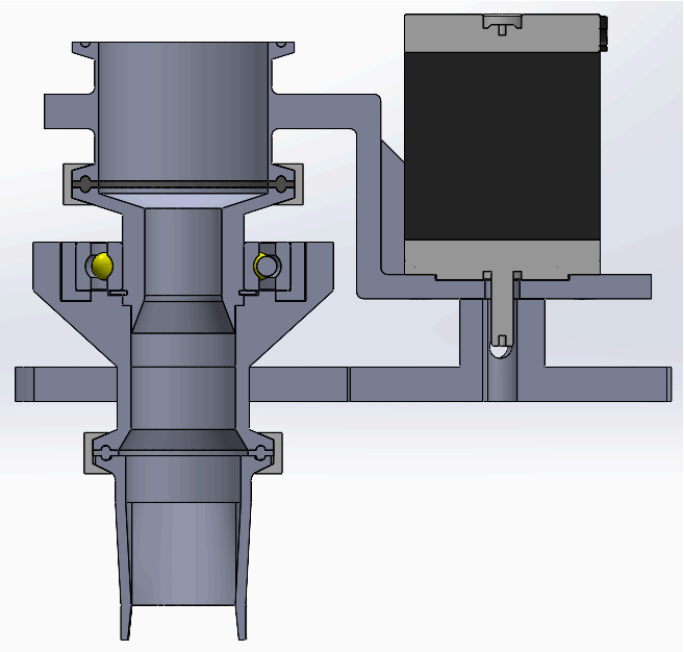

Figure 9: Section view of CAD model

A section view of the proposed CAD model and a detailed view of each part can be seen in Figure 9. The list of parts that have been integrated into nozzle can be found in Table 1:

Table 1: List of the rotating nozzle system parts

№	**Part Name**	**Quantity**	**Purpose**
1	*Lower adapter*	1	To joint nozzle head to the whole system
2	*Bearing Holder*	1	To fix outer ring of bearing
3	*Bearing*	1	Responsible for smooth rotation
4	*Gear (right) - pinion*	1	To transmit power from motor
5	*Motor holder*	1	To fix motor in stationary position
6	*Motor*	1	To provide rotation
7	*Nozzle head*	1	Replaceable part
8	*Clamp*	2	To connect two parts
9	*Upper adapter*	1	To fix bearing to stationary part of existing nozzle
10	*Snap ring*	1	To fix the bearing
11	*Gasket*	2	To prevent leaks

Due to the fact that the rotation system is designed from scratch and adapted to the parameters of the 3D printer, drawings of parts such as motor holder, lower short part, gear (right) - pinion and gear holder with output gear can be found in Appendix A.

3.4 Control Algorithm Development

The 3D printer works on *Duet3D* hardware, firmware and software basis. New rotating system is an open loop system which works with a separate motor which is controlled by a stepper driver. It was decided to use the *Nema 23* step motor and stepper driver *DM860*, because the same motor and driver are used to control the Z axis and extruder.

There is defined a new axis *U* which varies according to the printer motion in the X-Y (horizontal) plane and controlled by the new driver. The printer configuration is changed in accordance with the motor and driver characteristics with *RepRapFirmware Config Tool*.

The 3D printer for printing uses the G-code, a standard control language, of 3D model drawing. To obtain the G-code of the printing models for the construction printer, the *Simplify3D* Software is used. The software slices the 3D model into several layers. Each layer is then processed using the linearization principle, which calculates precise coordinates, defining the path and movement instructions for the printer head according to cartesian coordinates.

Overall, the 3D printer has counterclockwise printing motion. The nozzle rotation can be modeled by following figure:

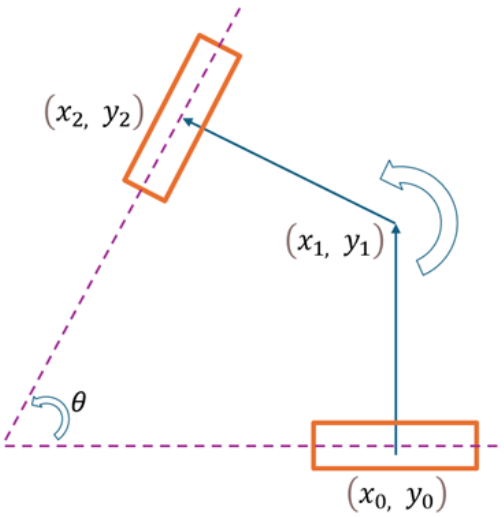

Figure 10: Rotating nozzle motion in X-Y plane:
orange box - nozzle head model, purple dashed line – axis of symmetry of nozzle head, blue vectors – printer head motion, Θ - rotation angle

According to Figure 10, the nozzle must rotate according to coordinates of three points: 0 - initial point, 1 - point of rotation, and 2 - final point. The angle of rotation can be described by the following mathematical model:

$$\theta = arccos\left(-\frac{(x_1-x_0)(x_2-x_1)+(y_1-y_0)(y_2-y_1)}{\sqrt{(x_1-x_0)^2+(y_1-y_0)^2}\sqrt{(x_2-x_1)^2+(y_2-y_1)^2}}\right) \quad (1)$$

U variable for G-code is identified according to the angle of rotation Θ and stepping characteristics of motor and driver. The printer extrudes material in a counterclockwise motion direction for circular shaped models, that is why the counterclockwise rotation has a positive angle of rotation, whereas the clockwise direction has a negative angle of rotation.

The rotating system control is developed according to specifications of the *Nema 23* motor. The motor has 1.8° stepping, each of which is subdivided into 16 steps by the driver. Overall, one step is equal to 0.1125° rotation, and one full 360° rotation requires 3200 steps. Simplified algorithm of control can be shown as follows:

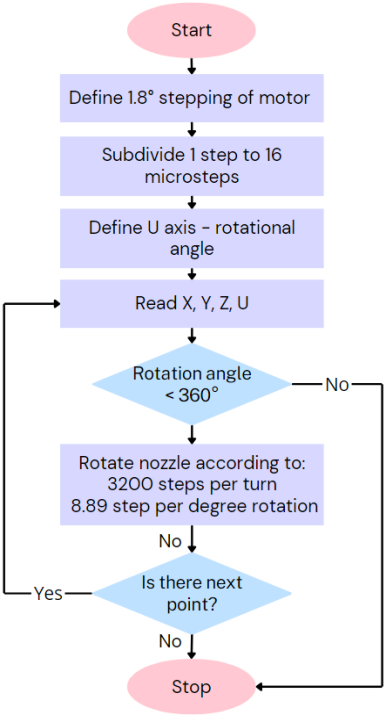

Figure 11: Control algorithm

3.5 Nozzle Design

For increasing the structural and mechanical properties of 3D-printed parts, nozzle design was varied from a standard circular nozzle to some geometries possessing unique forms. The crucial prerequisite in picking and designing all such nozzle geometries was that each of their proposed nozzle cross-sectional areas be the same as the reference circular nozzle to render equivalent material flow rate, extrusion pressure, and interlayer-bonding to ensure similarity between all of them. Using the formula for the area of a circle (eq. 2), the baseline circular nozzle area was computed:

$$A = \pi \times r^2 \tag{2}$$

The area with a radius of 10 mm was computed as follows:

$$A = \pi \times (10\,mm)^2 = 100 \times \pi \approx 314.16\,mm^2$$

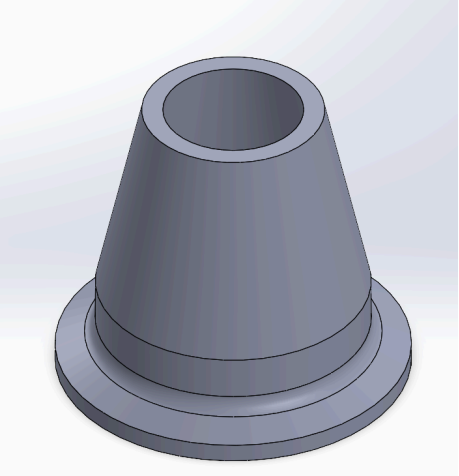

Figure 12: Circular nozzle

This area was targeted by every other alternative nozzle geometry, including rectangular, square, trapezoidal, rectangular with teeth, square, rectangular with one trowel, rectangular with two trowels, and rectangular with both trowels and teeth. Having this same constant cross-sectional area for all versions allowed a controlled comparative test so that variations in print quality, layer bonding, or mechanical strength noted could be largely the result of shape rather than material flow variation.

The rectangular nozzle profile's width and height were determined to be 22.8 mm and 13.8 mm, respectively. Their surface area of around 314 mm² (

$22.8\,mm \times 13.8\,mm \approx 314.64\,mm^2$) was enough to fit within the circular reference. Thus, they were selected. The toothed rectangular nozzle (Figure 13.a) was achieved through the addition of small protrusions along the longer edge (22.8 mm), and one or two incorporated trowel structures mounted along the shorter edge (13.8 mm) were included in the trowel versions (Figures 13.b and c respectively) . The trowels were designed to even out the surface of the extruded material, thus potentially increasing the interlayer adhesion and print quality. Cross-sectional area wasn't affected despite these additions, as trowels and teeth protrude outward from base dimensions and did not intrude into the interior flow space.

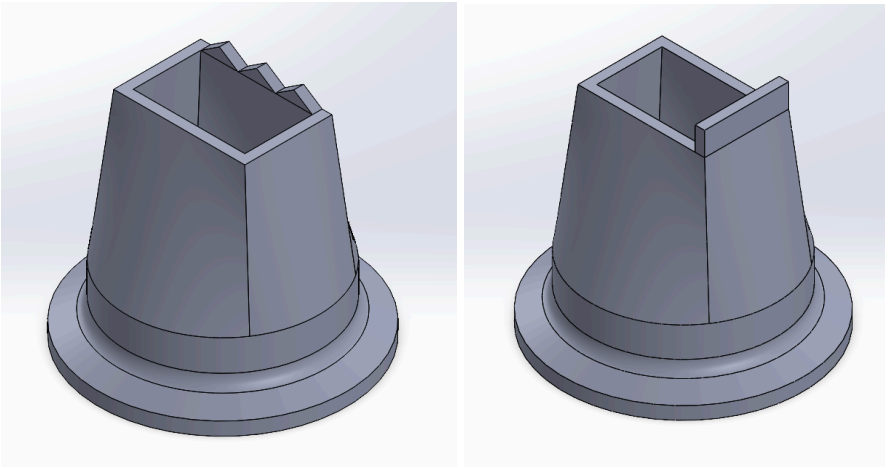

a) b)

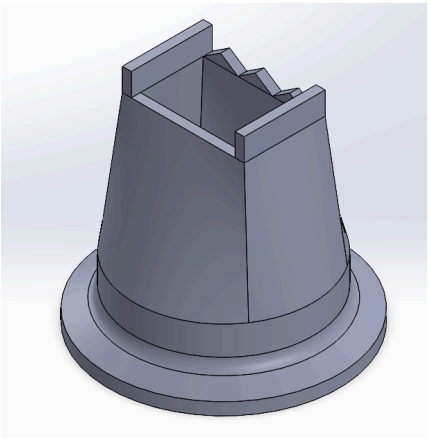

c)

Figure 13: Rectangular nozzles:

a) Teethed rectangular nozzle b) one trowel rectangular nozzle c) teethed and trowelled rectangular nozzle

For the square nozzle geometry (Figure 14), one side of 17.75 mm was calculated as $A = a^2 \rightarrow a = \sqrt{A} = \sqrt{314.16} \approx 17.72\,mm$ with minor adjustment to ease the manufacturing process. This provided a cross-sectional area of $17.75\,mm \times 17.75\,mm = 315.06\,mm^2$, again very close to the area of the circular nozzle. The square shape provided a flat flow profile and was primarily tested for its symmetry, which was believed to provide even layer deposition.

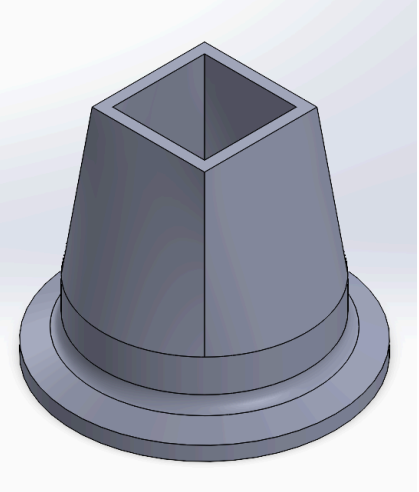

Figure 14: Square nozzle

The most geometrically complex of the shapes was the trapezoidal nozzle shape (Figure 15). It featured a longer base of 26 mm, a shorter upper side of 16 mm, and two equal sides of 15.81 mm. The trapezoidal nozzle dimensions were found using a trial and error method. The area of the trapezoid cross-section was calculated using the equation 3:

$$A = \frac{1}{2} \times (base\,1 + base\,2) \times height \quad (3)$$

$$A = \frac{1}{2} \times (26 + 16) \times 15 = 315\,mm^2$$

This dimension was slightly bigger than that of the circular reference area but within acceptable experimental tolerance, given the special mechanical properties the asymmetric shape might afford. For the trapezoidal nozzle with teeth, teeth were lined up along the longer base (26 mm), which enabled the design to achieve more surface engagement during the extrusion process. This design was particularly relevant to experiments that focused on improving the interfacial bonding of printed layers.

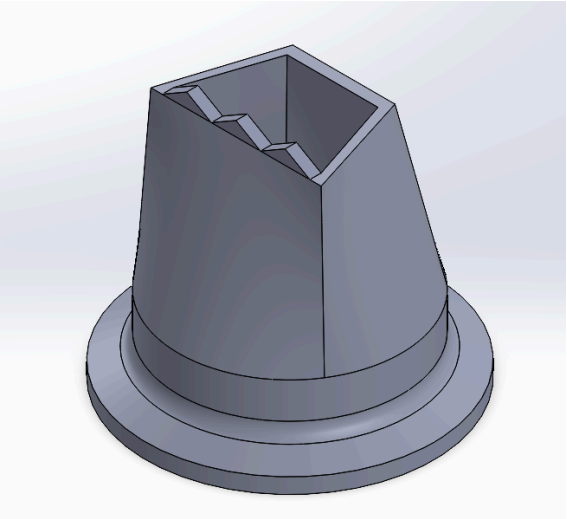

Figure 15: Trapezoidal teethed nozzle

For all the variations of nozzle geometries with the inclusion of features like teeth or trowels, it was necessary to preserve the internal flow geometry and therefore the cross-sectional area. This was achieved through the design of teeth and trowels such that they extended beyond the primary flow chamber. They changed the material deposition shape in this way without blocking or restricting the internal extrusion channel. Because of this precise control, changes to the nozzle geometry only affected the properties of surface interaction; flow coherence, extrusion pressure, or print velocity were never harmed.

All designs of nozzles were simulated in SolidWorks and integrated into the combined CAD model of the rotating nozzle system. The use of 3D models was utilized to simulate mechanical fit, structural alignment with the stepper motor and gear system, and spatial compatibility with the 3D printer's original stationary nozzle assembly. The modularity in design ensured easy interchangeability among nozzle types, making systematic experimental comparison possible. These nozzle geometries were then made using FDM 3D printing for testing and prototyping, with their performance evaluated in subsequent mechanical tests.

For a better insight into the performance impact of every nozzle geometry, extrusion tests were conducted. They were found to provide smoother top-of-layer surfaces due to mechanical smoothing provided by the trowel attachments but with slightly improved interlayer adhesion due to toothed nozzles, which caused micro-ridges to form, facilitating an improvement in the surface contact area. Print defects such as minor surface roughness would at times be observed on toothed nozzles, revealing an adhesion or visual finish trade-off.

The directional impact of introduced features in comparison with nozzle geometry was another critical observation. Teeth at the long sides and trowels at the short sides in a rectangular nozzle, as a specific example, helped achieve deposition control balancing and post-extrusion smoothing balance. Stabilized material shaping in both axes was guaranteed with such distribution. Similarly, the trapezoidal nozzle benefited by having its teeth on the more extended base to provide more contact during extrusion. These directional aspects were discovered to be significant in tailoring the nozzle design for specific printing purposes, such as maximizing strength, resolution, or surface finish.

3.6 Prototype Development

For fabrication of rotating nozzle model's parts such as gears, bearing housings, gear holder and motor mount 3D printing with fused deposition modeling (FDM) technology was used. This technology is the most cost effective and affordable during the initial stage of prototyping compared to other printing methods. Pictures of final printed parts can be found from Table 2 shown below:

Table 2: Pictures of manufactured parts

Picture of the part	Name
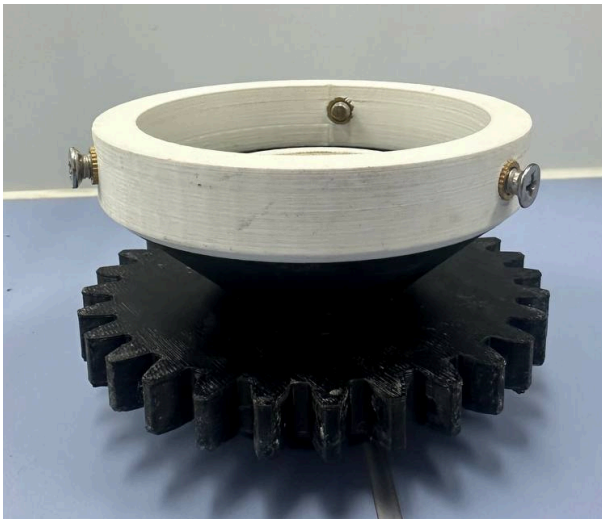	Lower adapter

Table 2 (continued): Pictures of manufactured parts

Picture of the part	Name
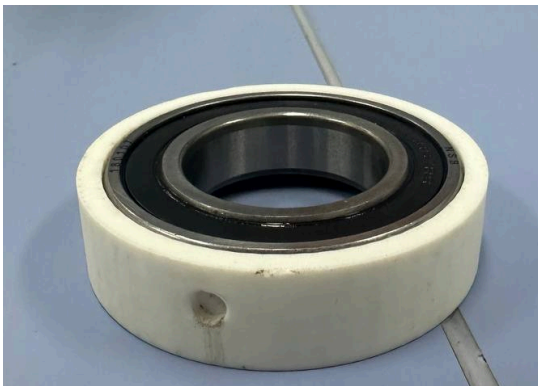	Bearing holder with bearing
	Upper adapter
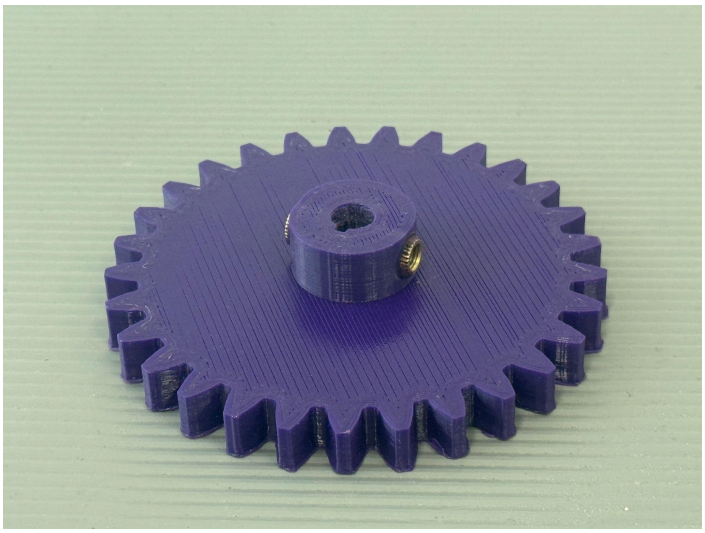	Gear (right) - pinion

Table 2 (continued): Pictures of manufactured parts

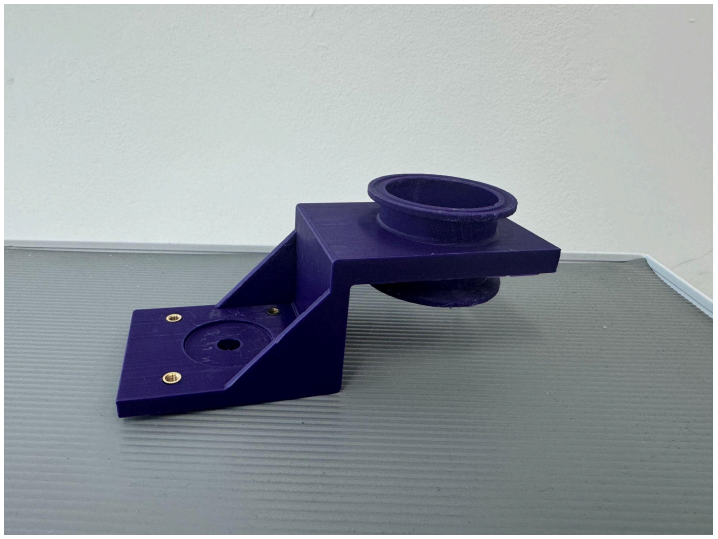	Motor holder

This rotational mechanical system is designed to ensure energy transfer and smooth rotation in the system. There are specific purposes of each component that are listed in Table 2:

- **Lower adapter** aims to connect the nozzle head with the rest of the system. Additionally there is an integrated gear system in the middle part of the lower adapter which is responsible for rotating the nozzle head.
- The second significant component of assembly is the **bearing holder with bearing** of 6007 type inside. Its purpose is to perceive rotational forces from the motor. Moreover, the bearing holder itself works as the holder of the bearing's outer ring, preventing it from shifting under load.
- The next component which is responsible for connecting fixed and moving parts of the whole system is the **upper adapter**. To be more precise, it keeps the bearing holder from falling with a snap ring. In addition the rest of the system is mounted on top of the bearing holder.
- **Gear (right)** which also operates as a **pinion** in the system, it aims to transmit motion and energy from motor to upper adapter's gear.
- The last part of the rotating mechanical system is the **motor holder**, which attaches the motor to itself and securely fixes it, since this part has a large mass due to the

motor. Because of this, the sides in the holder were made to stabilize and steady the system.

All the dimensions were created based on the existing default nozzle design of the 3D printer and adapted successfully to it. The proper assembly and timely maintenance of the rotational nozzle mechanical system is needed further to increase the durability and reliability of the system.

3.7 Printing Material Design

As the printing material used with the construction 3D printer is geopolymer mixture, that is considered to be a viscous material, it is essential to consider and investigate its rheological properties as it directly affects the printing outcomes. The preparation of the mixture is mixing of different materials together, thus it is a crucial step in the preparation of the geopolymer. It ensures proper distribution of reagents throughout the matrix and provides required chemical reactions for the geopolymer matrix to form. A well-designed mixing process ensures the desired functionality at the macro level. Each step of mixing is carefully designed to achieve optimal homogeneity and consistency in the resulting mixture.

In order to investigate and find the best possible ratio, iterative changes in one or several material proportions were used. Quantities of water, sand, clay, sodium silicate, GGBS, and metakaolin were some of the variables. The aim of this trial and error method was to find how the ratio of different materials affect the overall rheological properties such as flowability, workability or setting time as well as mechanical properties of the printed parts such as compressive and flexural strength or durability.

This trial-and-error technique was required to identify the optimum mix that satisfied both printability of the mixture and mechanical qualities of the produced parts. For the geopolymer mixture the following steps were followed:

Firstly, the metakaolin and sodium silicate are mixed together for 5 minutes at approximately 150-250 rpm. It is the primary and essential step that creates a base for the geopolymerization process to take place. The proper distribution of metakaolin particles in the sodium silicate makes it smoother and the polymerization reaction activates in a proper manner. Next step taken in order to prepare the geopolymer mixture is the addition of ground granulated blast furnace slag (GGBS) to the mixture of metakaolin and sodium silicate. After addition, the mixture is mixed for 3 minutes at 150-250 rpm. GGBS acts as a supplementary

cementitious material, directly affecting the setting of the whole mixture and its mechanical properties. Proper dispersion of GGBS ensures consistency in the mixture. GGBS is followed by the addition of sand and clay to the mixture. Sand and clay are added to the geopolymer in order to enhance its mechanical properties and workability of the fluid. Sand and clay are added and mixed for 5 minutes at 100-150 rpm. The last step is the addition of water to increase the fluidity of the mixture. This step needs a thorough physical examination of the mixture flowability and in cases of low fluidity the amount of water should be adjusted.

In summary, proper mixing is essential for achieving homogeneity, ensuring uniform distribution of ingredients, and promoting the desired chemical reactions in geopolymer recipes. Each mixing step contributes to the overall quality, performance, and suitability of the resulting geopolymer mixture for its intended application. Adjustments in mixing parameters, such as speed and duration, are carefully considered to optimize the properties of the geopolymer, including strength, workability, and durability. This meticulous approach to mixing is fundamental in producing high-quality geopolymers with consistent performance and reliability. As the mixture was used for 3D printing and all of the printed parts were used for the analysis of the results, such as compression test and rheology, proper mixing provides the accuracy of the printing and the results obtained. These results were used in order to create and find new proper recipes for the geopolymer mixture, changing the concentration of reagents and the reagents themselves.

3.8 Mechanical Strength Analysis

The effectiveness of usage of different non-circular nozzles is determined by comprehensive evaluation of the compressive strength and the flexural strength of the printed samples with comparison with molded samples. There are printed square shaped models with size 140x140x140 mm using optimized geopolymer mix as deposition material with 6 different nozzles. The layer height is 5 mm, the printing speed is 800 mm/min. The prints are cured at room temperature for 14 days for compressive and flexural strength testings.

The compressive strength testing shows the capacity of the printed structure to support the axial load. A higher compressive strength indicates that the printed material can support greater forces before failure occurs suggesting improved structural integrity. For the test, the printed models, after curing at room temperature, are cutted to cube shaped parts with approximate size 35x30x40 mm (see Figure 16).

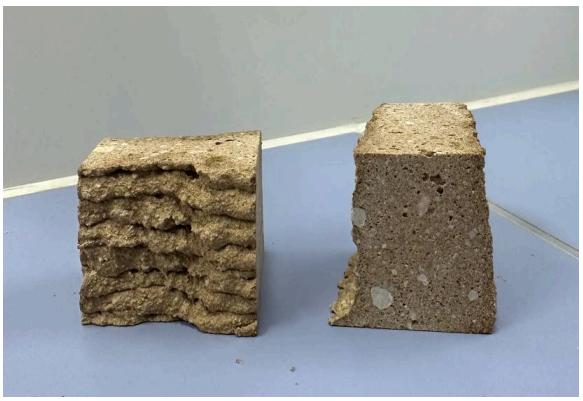

Figure 16: Compressive strength testing sample

On the 14th day of curing, they are tested on a compressive strength machine to identify the force which causes failure. The compressive strength is found according to equation 4:

$$P_c = \frac{F}{l*w} \tag{4}$$

where P_c - compressive strength, F - failure force, l - length of the sample,w - printing width. The obtained results are also compared with the compressive strength of the molded sample, which is the reference value that should be achieved within the framework of 3D printing.

The flexural strength testing identifies the ability of the printed model to resist bending load. The higher flexural strength shows overall resilience of the printed samples under tensile and bending loading. The flexural strength testing is done according to center point loading flexural test, that is why the printed samples are cutted along the layer with approximate size 40*30*120 mm (see Figure 17).

Figure 17: Flexural strength testing sample

On the 14th day of curing, they are tested on a center point loading flexural test machine to identify the force which causes bending failure. The flexural strength is found according to equation 5:

$$P_f = \frac{3F*l}{2*w*h^2} \quad (5)$$

where P_f - flexural strength, F - failure force, h - height of the sample. The obtained results are also compared with the flexural strength of the molded sample, which is the reference value that should be achieved within the framework of 3D printing.

3.9 Calendar Plan

The capstone project is done within the 2 semesters: Fall 2024 and Spring 2025.

The Fall 2024 semester is dedicated for the initial prototyping and first testing. The calendar plan for the Fall is given below:

Table 3: Calendar plan for Fall 2024

Fall 2024	August			September				October				November		
Week	1	2	3	4	5	6	7	8	9	10	11	12	13	14
Literature review														
Prototype design														
Manufacturing														
Assembly of the system														
Control algorithm development														
Integration to printer														
Testing for proper rotation														

The Spring 2025 semester is dedicated for the upgrading results from the Fall 2024, printing with geopolymer material and mechanical strength testings. The calendar plan for the Spring is given below:

Table 4: Calendar plan for Spring 2025

Spring 2025	January				February				March				April			
Week	1	2	3	4	5	6	7	8	9	10	11	12	13	14	15	16
Upgrade the design																
3D slicing renovation																
Upgrade the control algorithm																
Material composition optimization																
Develop design of different nozzle heads																
Printing and strength testing																
Discussion and analysis																
Report completion																

Chapter 4: Results

4.1 Overview

The experimental results demonstrate the development and the efficiency of the rotating nozzle design. Through iterative testing and performance analysis, this section validates the nozzle system's ability to enhance the mechanical properties of the printed structures, and determines the most worthwhile printhead design.

4.2 Mechanical System Assembly

As a result of designing, a working prototype of a rotating nozzle was created which can be seen from Figure 18. The rotation of the nozzle is provided by a system of two identical gears. The first one is driven by a motor, transmitting rotation to the second gear, which rotates the nozzle itself. The gear ratio 1:1 ensures uniform torque transmission and stable rotation of the nozzle. Each part of the assembly is connected to each other either by clamps from the existing nozzle, or by a threaded insert and a bolt.

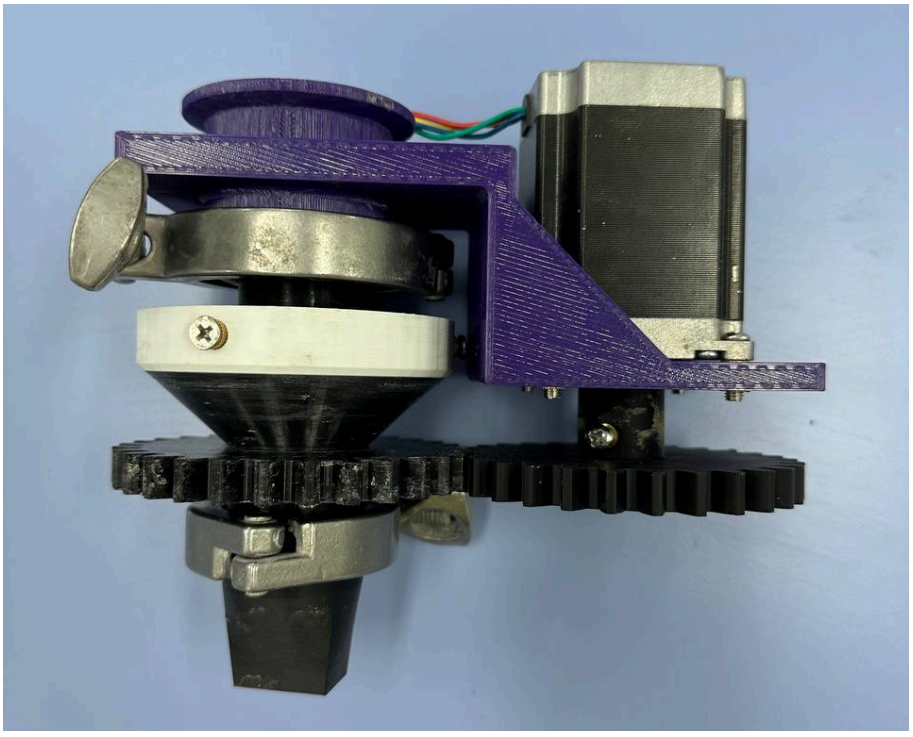

Figure 18: Assembly of mechanical system

The process of assembly begins with fit-pressing bearing of 6007 type into the bearing holder, where the inside diameter of the latter one is designed to be 0.5 mm less than the outer diameter of 6007 bearing. After that the bearing holder with bearing inside is set on the

upper adapter. On the bottom side of the upper adapter there is an attachment area where a snap ring is installed through a circlip plier tool. The purpose of this locking ring is to prevent axial displacement of the bearing. The upper adapter with the bearing holder is attached by a clamp (with a gasket between the two proposed connecting sides) to the fixed part of the 3D printer in the upper part.

Next is the connection of the lower adapter to the partially assembled system, or rather, to the bearing holder. This is done through three bolts, where the bolts are screwed into the upper adapter where the threaded bushings were installed. The bolts were taken 3 mm longer than the length of the threaded bushings so that the side 3 mm holes of the bearing holder could be secured. After that stepper motor is installed to the motor holder. The principle of fixing the motor is the same as in the lower adapter. So, firstly, 4 threaded bushings are soldered to four specified positions of the proposed bolt connection, then by placing the motor to its intended position four bolts are screwed. It allows the motor to be properly fixed. To the shaft of the installed motor, the right gear is installed by key to transmit the motion of the motor to the rest of the system. In addition, the height position of the right gear is adjusted by two bolts that compress the motor shaft on both sides. The correct alignment of the right gear (pinion) with the left is of great importance, since the rotational force is transmitted from the motor.

Finally, the nozzle head is connected by clamp to the rest of the system through a lower adapter. Moreover, a gasket is placed between nozzles and the lower adapter's connection area to prevent leakage and sliding.

The proposed design of the system and its reliability can be useful for applications that require controlled rotation. All parts of the system must be properly assembled and maintained to ensure optimal performance.

4.3 Control Algorithm Parameters

The updated configuration of the printer is given in Appendix B. There is defined by M569 command the driver, and by M584 command, the driver is bonded with the motor. After experimental testing of the performance for precise and smooth rotation with algorithm given in Figure 11, it is found that the driver controls the system with following optimal parameters:

- Maximum instantaneous speed changes: 0.9375 rpm, ensuring smooth transitions during rotation without introducing mechanical vibrations

- Maximum speeds: 9.375 rpm, which allows proper material deposition at point of rotation.

- Acceleration: 9.375 rev/s^2, securing accuracy and precision of the rotation speed and the rotation angle.

- Motor current: 2000 mA, selected to prevent overheating while providing sufficient torque for nozzle head rotation positioning under load.

The home parameter is a software-defined reference position similarly to the extrusion variable. Unlike X, Y, and Z control variables, which home position is also limited with a physical button, which defines origin, the extruder and the rotating nozzle do not have fixed origin position. After a new launch or each printing layer, the origin is resetted, and using cumulative data, there is initiated further motion.

So the *Duet3D* configurator could properly read and initiate motion defined by the G-code, and , there is added information about rotation angle, to the generated G-code by *Simplify3D,* according to Equation 1 and stepping size (1 step = 0.1125°) and speed of 30000 steps/s, which satisfies maximum speed limit of 9.375 rpm. There is provided an example (Ex. 1) of G-code for 90° rotation.

Example 1: Sample code

G92 E0.0000 U0.0000 ; reset extruder and the nozzle origin

G1 X413.200 Y313.200 F1800; home point-1

G1 X586.800 Y313.200 E43824.3522 F1440 ; point of rotation-1, home point-2

G1 U800 F30000 ; 90° rotation

G1 X586.800 Y486.800 E87648.7044 F1440 ; final point-1, new point of rotation-2, home point-3

G1 U1600 F30000 ;another 90° rotation

G1 X413.200 Y486.800 E131473.0565 F1440 ; final point-2, new point of rotation-3, home point-4

G1 U2400 F30000 ; another 90° rotation

G1 X413.200 Y313.200 E175297.4087 F1440 ; final point-3, new point of rotation-4,

G1 U3200 F30000 ; another 90° rotation

As shown in Example 1, the G92 command resets origin for the extrusion and rotation variables. The G1 command launch motion for stated parameters. Since rotation requires different speed, and it should be proceeded only on point of rotations (corners), the rotation

command is written as a separate line. 90° rotation is equal to 800 steps, and at the next corners, the rotation angle is given by cumulative values. At the same principle, other layer commands are updated.

4.4 Geopolymer Mixture

There is changed the material deposition shape in the way without blocking or restricting the internal extrusion channel. Because of this precise control, changes to the nozzle geometry only affected the properties of surface interaction; flow coherence, extrusion pressure, or print velocity were never harmed. This recipe was the most promising 3D printing recipe despite not achieving the same level of mechanical strength as conventionally molded samples.

Table 5: Geopolymer recipe

Composition	Ratio, gram
Mk	67.3
NaSil 55%	100
GGBS	20
Sand	137
Clay	45

Metakaolin (Mk), being the predominant aluminosilicate precursor, contributed significantly to the geopolymer matrix owing to its high reactivity and fine particle size, causing densification and structural cohesion. For the final recipe the nominal weight of the metakaolin is 67.3 grams. Sodium silicate (NaSil 55%) was the necessary alkali activator, which caused dissolution of the reactive aluminosilicates and initiated the geopolymerization reaction. Its nominal weight of 100 grams ensured an adequate amount of activation of both metakaolin and calcined clay, leading to a more cohesive and gel-like binder phase that enhanced the uniformity and extrudability of the mixture.

GGBS was added to increase the matrix with calcium to enhance the formation of additional binding phases and increase early strength gain. Although only 20 grams of nominal weight were added, this amount was optimized to improve the geopolymer reaction without making the mix too thick or interfering with print flow. Sand, weighing in ratio 137 grams, was employed as the primary aggregate and filler, adding bulk and dimensional

stability to the printed forms. It afforded the rigidity and deformation resistance required for multi-layer deposition during additively manufactured material. The 45 grams nominally weighted calcined clay also supported maintaining the matrix by increasing workability and contributing additional sources of alumina and silica to reaction. Its action on rheology was most beneficial in refining the viscosity of mixture to an acceptable balance between print integrity and extrudability.

Taken as a whole, the pieces created a thixotropic mix well suited for layer-by-layer creation. This mix exhibited print performance in bulk that was healthy overall with equable extrusion behavior and fluid deposition under all geometries used for a nozzle. The mix displayed pleasing buildability and resistance to distortion with extrusion. Nevertheless, despite these advantages, the mechanical tests revealed that both the compressive and flexural strengths of the printed samples were lower than those of molded reference specimens. This is due to the 3D printed material being anisotropic in nature and there being interlayer voids along with imprecise layer bonding between the deposited layers that reduce the continuity of the structure relative to the homogeneously cast molded samples.

4.5 Compressive and Flexural Strength

There are printed 6 square models with different nozzle shapes with optimized geopolymer mixture. As shown in Figure 19, rotation mechanism allows using different printheads that significantly affect the visual component of print walls. Each nozzle creates a unique texture and pattern, showing how much the nozzle shape can change the visual appearance of the print.

a. circular nozzle

b. square nozzle

c. rectangular nozzle with teeth

d. one trowel nozzle

e. trowels and teeth nozzle

f. trapezoidal nozzle

Figure 19: Print of square model with different nozzle heads

The printed models have a uniform layer height of on average 4.7±0.1 mm. The external wall size is 140±3 mm, while internal size differs according to nozzle head type. On average, the mass of each print is 4351 g.

The printed models are cured at room temperature. For compressive and flexural strength testings, the printed models are rock cutted so they are tested for the 14th curing day. The testing machine shows the amount of force in kN that leads to failure, and according to

Equation 1 and Equation 2, there are found the strength values in MPa for the printed samples. The results are given in Table 4.

Table 6: Mechanical strength of the samples on 14th day after printing

	Molded	Circular	Square	Teeth only	One trowel	Trowels and teeth	Trapezoidal with teeth
Compressive strength, MPa	15.65	6.03	6.24	7.39	7.21	7.57	7.78
Flexural strength, MPa	4.80	2.08	3.68	4.19	4.68	4.36	4.04

In the following Figure 20, there is shown visual representation of the compressive strength values, which describes the difference between values.

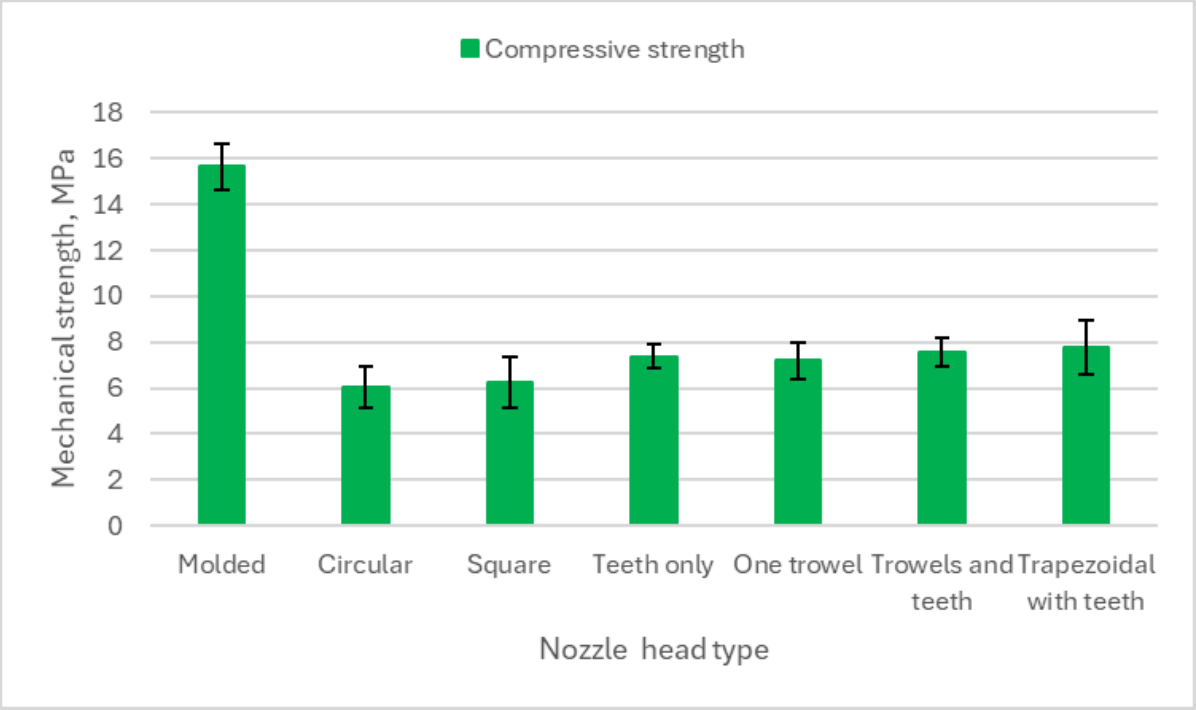

Figure 20: Comparison of compressive strength due to different nozzle usage

Generally, as expected, the highest compressive strength is given for the molded sample, and it is the reference value. The default print with circular sample has compressive strength lower by 61.5%. The highest compressive strength originated with trapezoidal with teeth shaped printhead, which has the strength 29.0% higher than the circular nozzle samples, and only to 50.3% less than the reference value. Square shaped nozzle causes a slight increase in compressive strength relative to the circular nozzle, however the usage of other types of nozzle heads significantly improve the compressive strength of printed models.

In the following Figure 21, there is shown visual representation of the flexural strength values, which describes the difference between values.

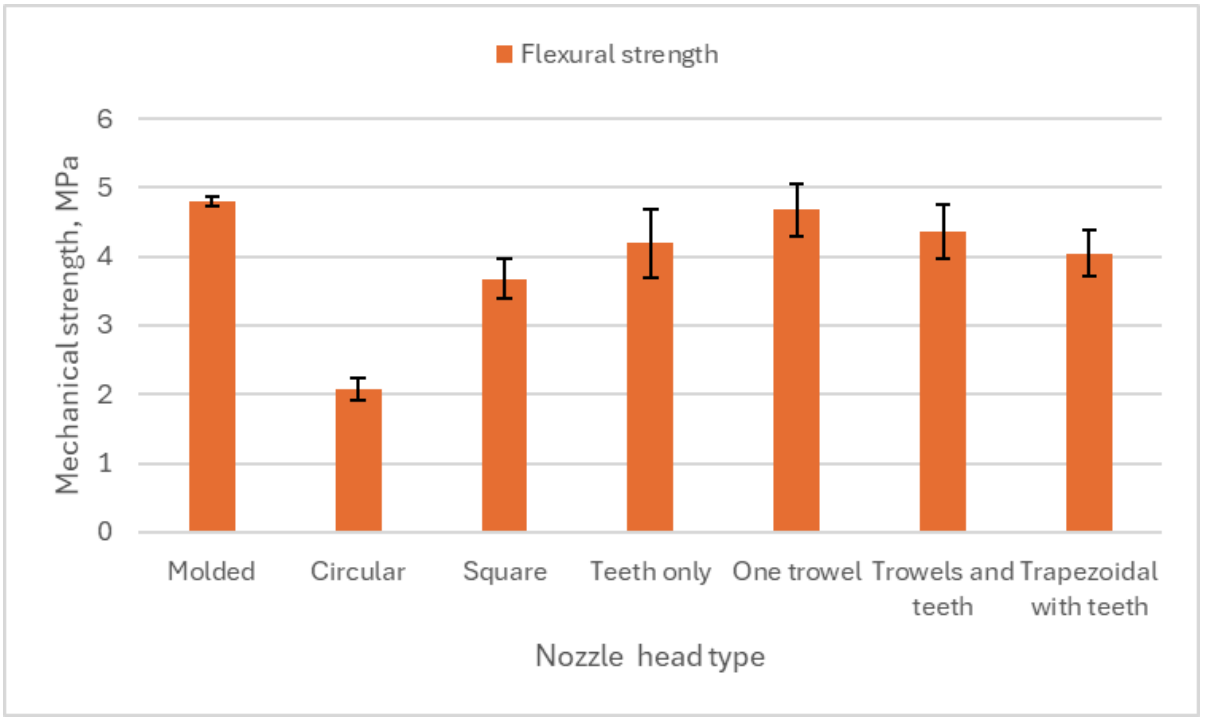

Figure 21: Comparison of flexural strength due to different nozzle usage

The highest flexural strength is given by the molded sample value, and is set as the reference value. The default print with circular sample has flexural strength lower by 130.8% relative to reference value of molded samples. The highest flexural strength originated with one trowel printhead, which has the strength 125.0% higher than the circular nozzle samples, and only to 2.5% less than the reference value. The usage of noncircular types of nozzle heads significantly improve the flexural strength of printed models.

Chapter 5: Discussion and Analysis

5.1 Overview

According to the proposed design, the rotating nozzle system was successfully assembled, incorporating all essential components necessary for its operation. The assembly was followed by rigorous testing to verify the system's mechanical functionality and its ability to perform accurate rotational movements at various angles.

5.2 Design Challenges

Two major issues have been encountered during the printing process with a non-circular nozzle. The first problem was the detachment of the white lower adapter from the purple bearing holder as shown in Figure 22.

Figure 22: Detachment of lower from upper adapter

This separation occurred because of the fact that the connection between these two components were insufficiently reinforced. As a result, the partial-depth holes of 3 mm in the bearing holder were made in 3D design to resolve the above mentioned problem. One of those made holes can be seen from Figure 23. This modification provides a more secure mounting point for the lower adapter and a tighter mechanical connection between it and the bearing holder.

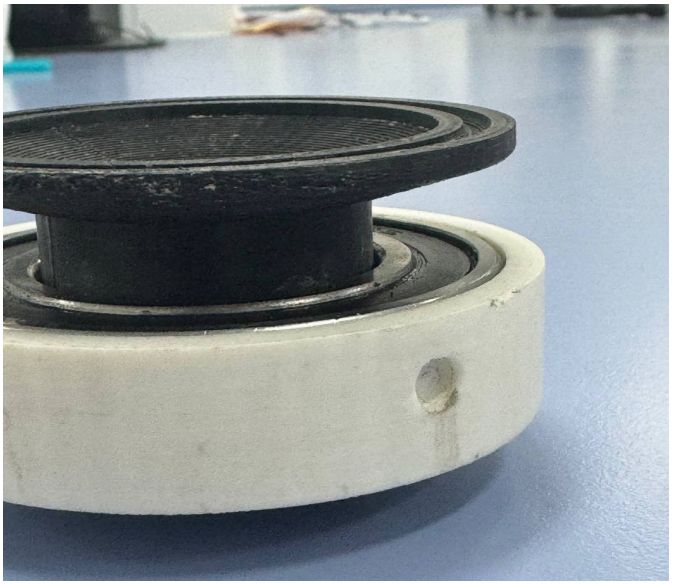

Figure 23: Partial-depth holes of 3 mm in the bearing holder

The second problem, illustrated in Figure 24 and 25, was the failure of the upper adapter section, to be exactly, the area where the snap ring was attached.

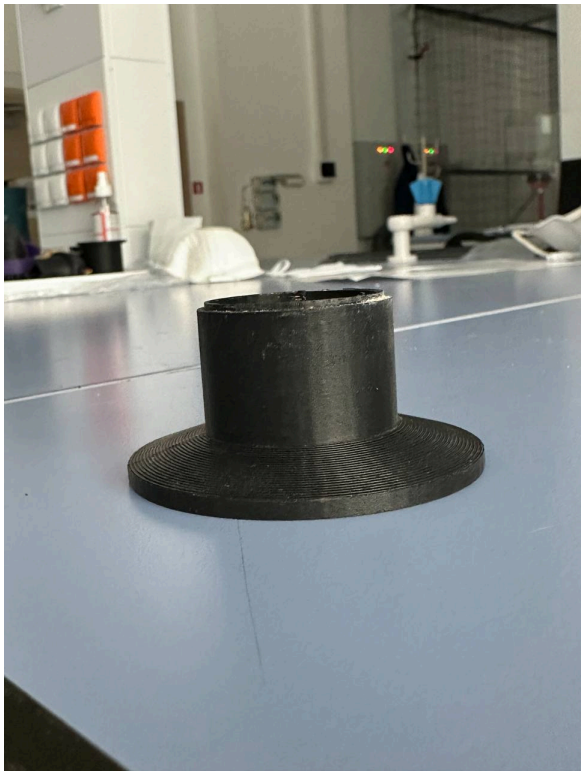

Figure 24: The broken upper adapter part (downside)

Figure 25: The broken upper adapter part (upside)

It was caused because of the significant amount of stress on this area. To address this issue the affected part was redesigned including increase of both width and length dimensions of the snap ring attachment area. This allows to distribute mechanical stress evenly which can reduce the probability of fractures and improve the durability of the upper adapter.

Both solutions focus on reinforcement of critical connection areas. The purpose of modifications was not only to fix the immediate problem by just reprinting broken parts with previous dimensions but also to contribute to its long-term reliability by making significant minor adjustments. Finally, the structural integrity of the entire system has been enhanced.

5.3 Material Design Challenges

Despite the fact that the geopolymer paste composition is kept at constant ratio there were adjusted clay, sand and water proportions. The optimization of the geopolymer mortar composition is essential for high quality printing which has stable structure and uniform layer height without losing its structural integrity.

A geopolymer mortar made with a sand:clay:water ratio of 125:45:6 was used for the initial print test. Because of the relatively high viscosity this mixture produced, the material was less flexible during the printing process but more resistant to flow. Although the first layers were successfully deposited, considerable bending stress was introduced by the subsequent layers' growing weight during printing. Due to limited interlayer adhesion and inadequate structural stability, the printed structure started to deform, as shown in Figure 26. After the 14th layer, the structure finally failed due to its inability to support the weight from the upper layers. This result demonstrated the necessity of further mixture optimization by raising the proportion of coarse aggregate and lowering the proportion of water in order to improve the buildability of the structure.

Figure 26: The print with geopolymer with sand:clay:water ratio of 125:45:6

The geopolymer mortar mix for the second printing attempt was adjusted to a 137:45:6 sand:clay:water ratio that included more sand but the same respective ratio of clay and water. The following Figure 27. depicts how much more stable the structure was than the first attempt. The entire print came out well without failure, and the printed layers kept their shape more. However, the geopolymer mixture was not hard enough to withstand bending, that is why the walls were printed in bended shape.

Figure 27: The print with geopolymer with sand:clay:water ratio of 137:45:6

In the third print test geopolymer mortar was formed based on the mix with the ratio of sand:clay 137:45, but excluding the added water. This change led to reduction in the viscosity of the mortar and better building up of the layer deposition. As seen in the Figure 28, this composition gave the most favorable structural performance among all the tests. The walls of the printed specimen were straight and rigid in each layer formed and there was no remarkable difference in the height of each layer. This coarse aggregate ratio is kept for further printings.

Figure 28: The print with geopolymer with sand:clay ratio of 137:45

5.4 System Operation

Figure 29: Front view of the installed assembly

The development and testing of the rotating nozzle system brought forth some key findings and challenges that have important implications for improving the 3D printing in construction. The assembled rotating nozzle system demonstrated the capability of accurate rotational control with angles of 90°, 180°, 360°, and 720°. These results confirm the feasibility of a rotational mechanism integrated into a 3D construction printer, which could make dynamic adjustments of the nozzle for different geometries. The addition of the U-axis to the configuration of the printer is another new contribution to 3D printing technology. During testing, the system demonstrated fluent and precise rotation.

The test on appropriate rotation provided insight into how the system was performing. For speeds less than 3.125 revolutions per minute, it failed to rotate; optimal working occurred at 9.375 revolutions per minute at an acceleration of this same value. It was noticed that the repeated call of the same angle does not cause repeated rotation. The system asks to call a new angle. It happens due to sensitivity on cumulative value of angle - absolute position relative to initial. It does not turn again because the nozzle is already positioned at that angle. However, calling another angle causes the system to reset the initial position, which leads to proper rotation of the nozzle.

Prolonged testing also led to heating of motors up to 83° C which, in future, may lead to deformation of the system. To resolve this issue, the dynamic current setting of the driver was adjusted. This was accomplished by activating the DIP switches SW4, SW5, and SW6, as outlined in the DM860H manual (n.d.). This modification effectively resolved the overheating problem, so repeated tests have shown that the motor heats up 28° C.

5.5 Effect of Nozzle Head Shape

The rotating nozzle system allows usage of different nozzle heads for reaching different design and mechanical properties. According to the results at section 4.4, each nozzle affects the visual structure of the printed object, and to its mechanical properties, specifically the compressive and flexural strength.

According to Figure 19.a, the circular nozzle deposits material in the way where each layer has a convex shape. By using a square nozzle as in Figure 19.b, on the other hand, the surface quality is enhanced, enabling the deposition of each layer with a more uniform and smooth profile. The rectangular nozzle with teeth has a similar effect as the square nozzle showing in Figure 19.c, however the teeth influence the adhesion between layers. The usage of a nozzle with a single trowel as in Figure 19.d, which trowel glides along the outer wall, makes smooth wall structure, but it does not make a smooth inner wall. The nozzle with two trowels and teeth, in contrast, effectively creates smooth inner and outer walls (see Figure 19.e), leading to a more smooth straight surface. Lastly, the trapezoidal nozzle, as in Figure 19.f, produces more distinct and consistently separated layers because of its design, which results in uneven material deposition over the layer width.

Overall, the choice of nozzle design has a significant impact on the surface quality and aesthetic characteristics of printed structures. Circular nozzles tend to produce convex layers, while square and rectangular nozzles improve surface uniformity and layer smoothness. Features such as teeth and trowels further enhance adhesion between layers and the smoothness of both inner and outer walls. Meanwhile, trapezoidal nozzles can create visually distinct, though less uniform, layers. Therefore, careful selection of nozzle geometry allows for optimization of both mechanical performance and the visual appearance of printed objects, depending on the specific application requirements.

The variation in mechanical strength across different nozzle types clearly demonstrates that nozzle design plays a critical role in influencing the overall performance of printed structures. As illustrated in Figure 20, the use of noncircular nozzles leads to an increase in compressive strength by at least 3.5%, an improvement primarily attributed to printing with a square-shaped nozzle. This suggests that even minor deviations from default circular nozzle designs can positively impact the structural integrity of printed materials. Furthermore, nozzle heads equipped with teeth show a remarkable enhancement in compressive strength, achieving gains between 22.6% and 29.0% relative to the standard circular nozzle. This substantial improvement indicates that the addition of mechanical features such as teeth helps in better compaction and interlayer bonding during the printing process. Similarly, nozzles featuring a trowel attachment also contribute to a notable increase in compressive strength, improving it by approximately 19.5%.

Turning to the flexural strength, Figure 21 presents further evidence of the benefits of alternative nozzle designs. The usage of noncircular nozzles increases the flexural strength by at least 16.3%, again most notably when employing the square-shaped nozzle. Moreover, nozzle heads fitted with one or more trowels lead to an even more impressive improvement in flexural strength, enhancing it by between 41.6% and 51.9% compared to circular nozzles. This dramatic rise highlights the effectiveness of trowel features in distributing stresses more evenly across the material, thus improving its ability to resist bending forces. Additionally, nozzle designs incorporating teeth also yield significant flexural strength benefits, with increases ranging from 31.2% to 36.0%.

Generally, it can be summarized that nozzle heads featuring teeth are particularly effective in significantly boosting the compressive strength of printed objects, likely due to their ability to promote better layer adhesion. In contrast, nozzles equipped with trowels are especially beneficial in enhancing the flexural strength of printed models, likely due to their influence on shaping and smoothing the extruded material, resulting in improved structural uniformity and resistance to bending stresses.

5.6 Cost Analysis

The total cost for all required components in this assembly amounts to 62 USD. The largest expenses are the NEMA motor of 35 USD and 1 kilogram of PLA plastic material of 23 USD. This plastic will be used to create the main components of assembly. Other needed components include a 6007 type bearing, 10 bolts, 10 threaded bushings, and snap ring priced each at 1 USD. This combination of components keeps costs low while still making everything working correctly. The bill of materials can be found from Table 5. The prices are considered according to the *Amazon.com* market.

Table 7: Cost analysis

№	**Part Name**	**Quantity**	**Price**
1	*Plastic PLA, kg*	1	23$
2	*Bearing 6007, piece*	1	1$
3	*Motor Nema, piece*	1	35$
4	*Bolt, piece*	10	1$
5	*Threaded bushing, piece*	10	1$
6	*Snap ring, piece*	1	1$
	Total		62$

Chapter 6: Conclusion and Further Research

6.1 Conclusion

This report discussed a capstone project targeting the improvement of a new rotating nozzle system for addressing the shortcomings of a stationary circular nozzle in the construction 3D printers industry. The design would include rotational capability, non-circular geometries to increase adaptability and improve the mechanical characteristics of the parts printed. Printing tests have been conducted with the 6 nozzle designs, namely Square, Teeth only, One trowel, Trowels and teeth, Trapezoidal with teeth, and Circular (default one). The major developments and results of this capstone project are a precise control system, a modular mechanical design, effective assembly of the revolving nozzle mechanism, establishment of the best nozzle design through compressive and flexural testing and performance evaluation.

6.2 Contribution to Knowledge

Key testing objectives were to establish that the nozzle rotation was mechanically operational, compatible with the current configuration of the 3D printer and improvement of mechanical properties of printed material by a new rotational mechanical system. All of these objectives were reached and fulfilled. Based on testing results one trowel printhead had the highest flexural strength which is approximately 5 MPa while for the circular nozzle this value is only 2 MPa, which is 2.5 times less. Additionally a trapezoidal printhead with teeth had the highest compressive strength of 8 MPa compared to the default circular nozzle with 6 MPa. These results have explicitly demonstrated precise rotational control, the advantages of a rotational mechanical nozzle system over the default circular nozzle of a 3D printer and a solid foundation for future performance evaluation.

6.3 Further Research

In further stages, more tests should be done in order to evaluate the influence of the other type of spinning nozzle on the quality of the print, on the interlayer bonding, and on the general structural performance.

In general, it is possible to implement rotational mechanisms within the nozzles of construction 3D printers, as was demonstrated with this project. Although the realization of large-scale 3D printing in construction needs more tests and optimization to reach its full potential, this work represents an important step toward the enhancement of such technology

in terms of efficiency, sustainability, and versatility. Results from this project create further room for investigation and contribute to the development of the 3D printer technology in construction.

References

Almutairi, A. L., Tayeh, B. A., Adesina, A., Isleem, H. F., & Zeyad, A. M. (2021). Potential applications of geopolymer concrete in construction: A review. *Case Studies in Construction Materials*, *15*, e00733. https://doi.org/10.1016/j.cscm.2021.e00733

BigBolt. (2022, February 2). What Are The 7 Steps Of The Engineering Design Process. *Go Big Bolt*. https://www.gobigbolt.com/blog/step-engineering-design-process

Cong, P., & Cheng, Y. (2021). Advances in geopolymer materials: A comprehensive review. *Journal of Traffic and Transportation Engineering (English Edition)*, *8*(3), 283–314. https://doi.org/10.1016/j.jtte.2021.03.004

Duxson, P., Fernández-Jiménez, A., Provis, J. L., Lukey, G. C., Palomo, A., & Van Deventer, J. S. J. (2006). Geopolymer technology: the current state of the art. *Journal of Materials Science*, *42*(9), 2917–2933. https://doi.org/10.1007/s10853-006-0637-z

He, L., Tan, J. Z. M., Chow, W. T., Li, H., & Pan, J. (2021). Design of novel nozzles for higher interlayer strength of 3D printed cement paste. *Additive Manufacturing*, *48*, 102452. https://doi.org/10.1016/j.addma.2021.102452

Manikandan, K., Jiang, X., Singh, A. A., Li, B., & Qin, H. (2020). Effects of nozzle geometries on 3D printing of clay constructs: quantifying contour deviation and mechanical properties. Procedia Manufacturing, 48, 678–683. https://doi.org/10.1016/j.promfg.2020.05.160

Rasiya, G., Shukla, A., & Saran, K. (2021). Additive Manufacturing-A Review. Materials Today Proceedings, 47, 6896–6901. https://doi.org/10.1016/j.matpr.2021.05.181

Shakor, P., Nejadi, S., & Paul, G. (2019). A Study into the Effect of Different Nozzles Shapes and Fibre-Reinforcement in 3D Printed Mortar. Materials, 12(10), 1708. https://doi.org/10.3390/ma12101708

User's Manual For DM860H Fully Digital Stepper Drive. (n.d.).

Xiao, J., Ji, G., Zhang, Y., Ma, G., Mechtcherine, V., Pan, J., Wang, L., Ding, T., Duan, Z., & Du, S. (2021). Large-scale 3D printing concrete technology: Current status and future opportunities. *Cement and Concrete Composites*, *122*, 104115. https://doi.org/10.1016/j.cemconcomp.2021.104115

Yang, L., Sepasgozar, S. M., Shirowzhan, S., Kashani, A., & Edwards, D. (2022). Nozzle criteria for enhancing extrudability, buildability and interlayer bonding in 3D printing concrete. *Automation in Construction*, *146*, 104671. https://doi.org/10.1016/j.autcon.2022.104671

Appendix A. Drawings of the rotating nozzle system

A.1 Gear Holder with output gear

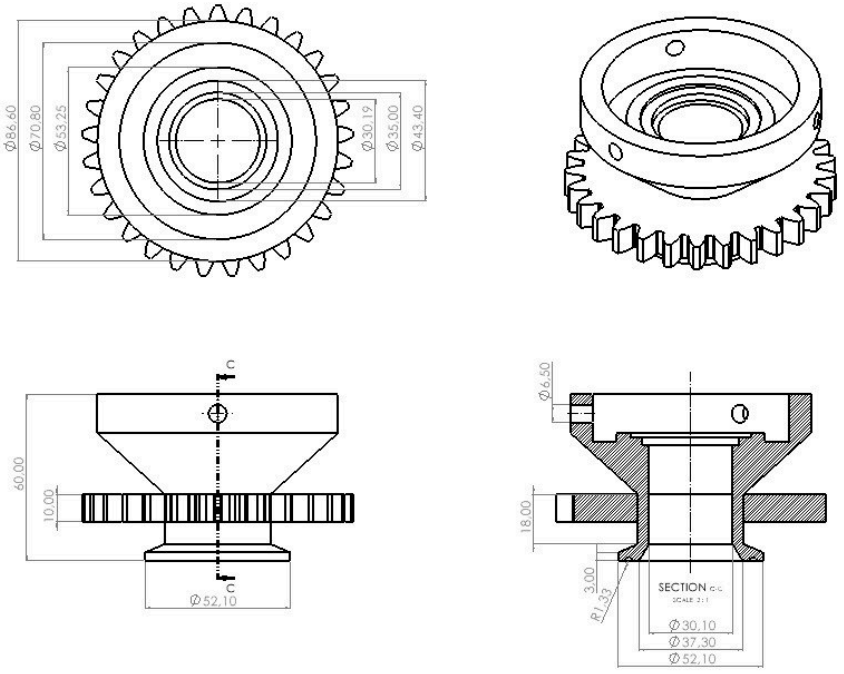

A.2 Lower short part

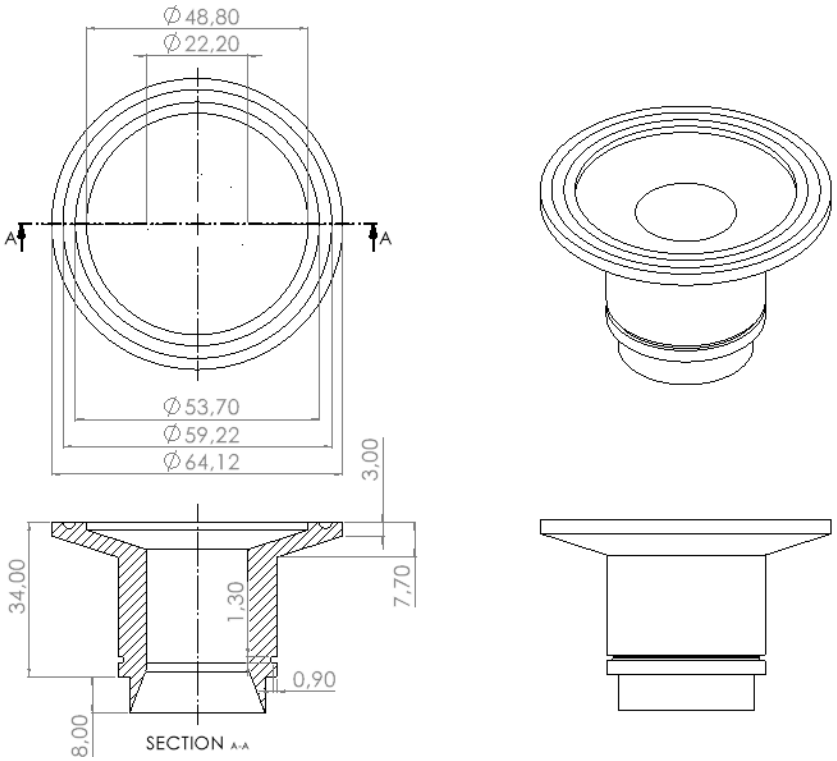

A.3 Motor Holder

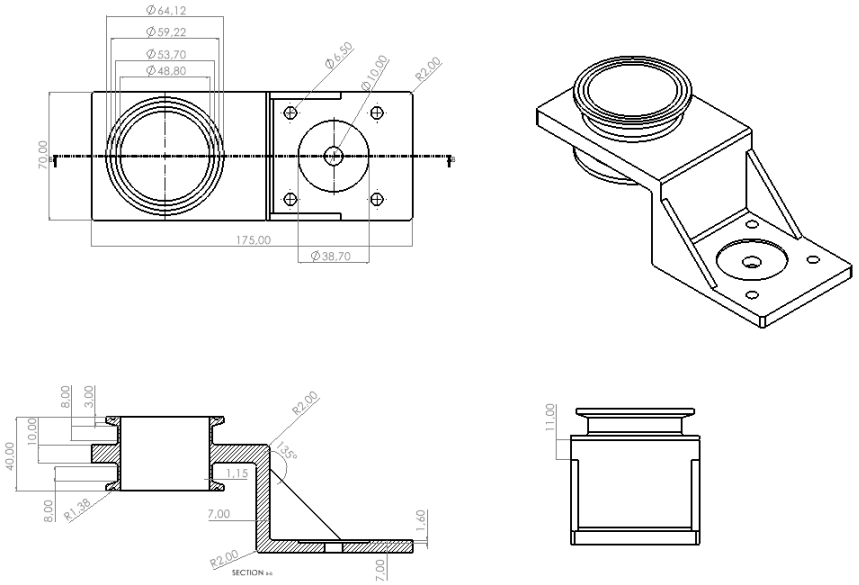

A.4 Gear (right) - pinion

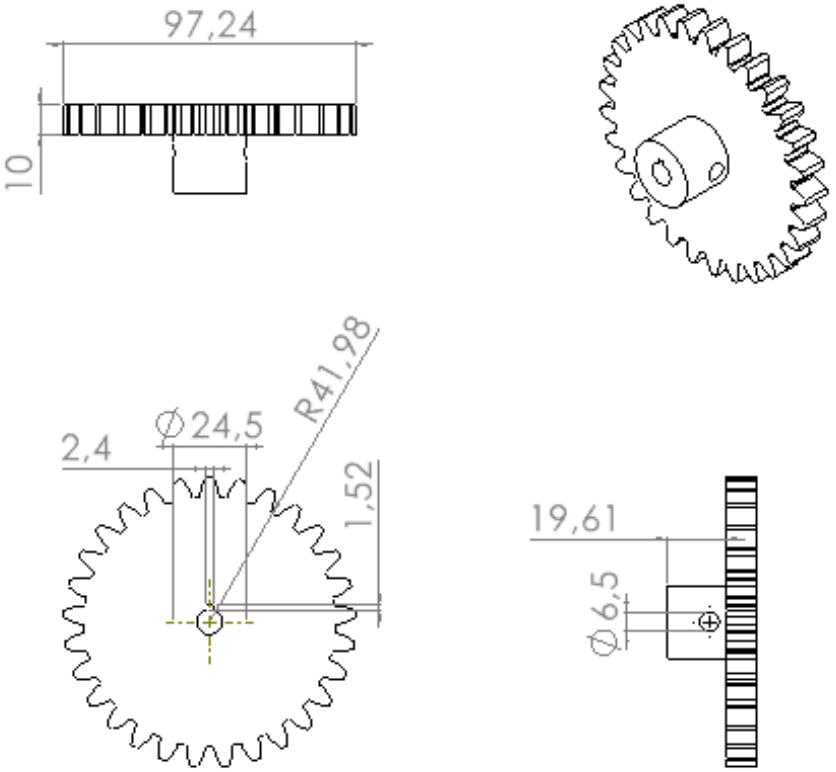

Appendix B. Configuration file.

```
; Configuration file for factory testing Duet Ethernet and Wifi with V2.01 firmware

G21                                     ; Work in millimetres
; General preferences
G90                                ; Send absolute coordinates...
M83                                ; ...but relative extruder moves

; Network
M111 S0                            ; Debug off

M550 PStoneFlowerMortar            ; Set machine name
M551 StoneFlowerMortar             ; Machine password (used for FTP)
M552 S0                       ; Enable network
M552 S1                       ; Enable network
M586 P0 S1                         ; Enable HTTP
M586 P1 S0                         ; Disable FTP
M586 P2 S0                         ; Disable Telnet

; Drives
M569 P5 S1                    ; Drive 5X goes forwards
M569 P6 S1                    ; Drive 6Y goes forwards
M569 P2 S1                    ; Drive 2Z goes backwards
M569 P7 S0                    ; Drive 3 goes forwards E0
M569 P8 S0                    ; Drive 4 goes forwards E1
M569 P9 S0                    ; Drive 5 (mortar pump) goes backwards E2

M584 Z2 X5 Y6 U7 E8:9; axes

configuration (all endstops at high end, active high)
;*** The homed height is deliberately set too high in the following - you will adjust it during
calibration active high

M350 X16 Y16 I0                    ; Configure microstepping with interpolation
M350 Z16 I1
M350 U16 E16:16 I0                 ; Configure microstepping without interpolation
M92 X33.68 Y33.68 Z1357.58 U8.889 E62.50:10.42;     ; number of steps per mm filament
2.5mm, Ram L, Z axis 12x3, angle in grad
M566 X2000 Y2000 Z1000 U500 E100000:100000     ; Set maximum instantaneous speed
changes (mm/min)
M203 X4000 Y4000 Z2000 U10000 E1000000:1000000   ; Set maximum speeds (mm/min)
M201 X500 Y500 Z500 U1000 E1000000:1000000    ; Set accelerations (mm/s^2)
M906 X2000 Y2000 Z2200 U2000 E1000:1000 I30      ; Set motor currents (mA) and motor
idle factor in per cent
M84 S30                            ; Set idle timeout

; Axis Limits
M208 X0 Y0 Z0 U0 S1                ; Set axis minima
M208 X1500 Y800 Z600 U10000 S0                  ; Set axis maxima
```

```
; Endstops
M574 X1 Y1 Z1 S1                        ; Set active high endstops

; Z-Probe
M558 P1 H5 F120 T6000   ; Set Z probe type to unmodulated and the dive height + speeds
G31 P500 X0 Y0 Z2.5             ; Set Z probe trigger value, offset and trigger height
M557 X15:465 Y15:465 S20                        ; Define mesh grid

; Heaters
M140 H-1                                ; Disable heated bed

; Fans
M106 P0 S0.3 I0 F500 H-1                        ; Set fan 0 value, PWM signal inversion and
frequency. Thermostatic control is turned off
M106 P1 S1 I0 F500 H-1                          ; Set fan 1 value, PWM signal inversion and
frequency. Thermostatic control is turned off
M106 P2 S1 I0 F500 H-1                          ; Set fan 2 value, PWM signal inversion and
frequency. Thermostatic control is turned off

; Tools - rotating nozzle tool
M563 P0 D0                      ; Define tool 0, use Extruder 1
G10  P0 X0 Y0 Z0 U0                     ; Set tool 0 axis offsets
G10  P0 R0 S0                   ; Set initial tool 0 active and standby temperatures to 0C
M567 P0 E1.0                ; Run ram at speed 1 ram extruder 1 at normal speed 1.0
M568 P0 S0                      ; Enable color mixing
T0                              ; Select tool T0
M302 P1                         ; allow cold extrusion

; Tools
M563 P1 D0:1     ; Define tool 0, use Extruder 0, Extruder 1, Pump 2 and no heater
G10  P0 X0 Y0 Z0                    ; Set tool 0 axis offsets
G10  P0 R0 S0                   ; Set initial tool 0 active and standby temperatures to 0C
M567 P0 E1.5:1.0            ; Run print head 0 at speed 1.5, ram extruder 1 at normal speed 1.0
M568 P0 S0                      ; Enable color mixing
T1                              ; Select tool T1
M302 P1                         ; allow cold extrusion

; Tools
M563 P2 D0:2            ; Define tool 1, use Extruder 0, Extruder 1, Pump 2 and no heater
G10  P1 X0 Y0 Z0                    ; Set tool 0 axis offsets
G10  P1 R0 S0                   ; Set initial tool 0 active and standby temperatures to 0C
M567 P1 E0.1:0.235544           ; Run print head 0 at speed 0.1, pump at normal speed 0.23554
M568 P1 S0                      ; Enable color mixing
T2                              ; Select tool T1
M302 P1                         ; allow cold extrusion

T0                              ; Select tool T0
```